NOTE

Invasive ants of tropical origin at mid-high altitude and latitude: adaptation and invasiveness

(Laboratory of Ecosystem Management and Conservation Ecology, RISH, Kyoto University)

Chin-Cheng Yang and Yi-Ming Weng

Abstract

Recent discovery of longhorn crazy ant (*Paratrechina longicornis*) at mid-high altitude and latitude raises a series of ecological and evolutionary issues as this invasive ant, although reportedly originated from tropical regions, seems to be able to survive through cold environments. We thus are interested in understanding if colonization of longhorn crazy ant into these areas involves thermal adaptation, and if such adaptive potential results from behavioral/physiological plasticity or strong genetic basis. Here we reported some preliminary data and also presented future research framework of my laboratory on dissecting the adaptive mechanisms of this invasive ant. Results are expected to serve baseline information for development of management strategy on ant invasion under different temperature regimes.

Introduction

Tropical regions have been regarded as one of the top ‘‘source population’’ hotspots for quite a few invasive ants. These ant species include *Paratrechina longicornis* (longhorn crazy ant, LCA), *Anoplolepis gracilipes* (yellow crazy ant, YCA), *Solenopsis geminata* (tropical fire ant, TFA), *Pheidole megacephala* (African big-headed ant, ABA) and *Monomorium destructor* (Singapore ant, SA), all of which have been transported around the world from the tropics where they are native and have become major ecological, agricultural, and/or household pests in most of areas they were introduced into [1].

Taking LCA as an example, most of LCA samples were collected in low-elevation areas including cities and suburbs where human activities are generally intense (Fig. 1). Such distributional pattern not only is in perfect agreement with the prediction that this ant has originated from the tropics but also verifies the preference of warmer habitats by LCA. However, recent collection efforts of our lab revealed a surprising finding that a handful of LCA samples were discovered in mountain areas with mid-high elevation (600-1200 m) in northern Taiwan (Fig. 1), leading us to hypothesize that colonization of mid-high elevation by LCA may have involved adaptation to cold environments. Hence, this study represents a first attempt to test if such thermal adaptation exists for LCA.

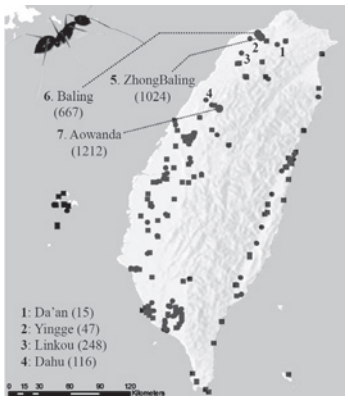

Figure 1. Map showing various collection sites of LCA in Taiwan. Nests used in the chill coma recovery experiments were collected from Site 1~7. Number in parenthesis indicates the elevation (m) of a given LCA nest was collected.

Materials and methods

We collected a total of seven LCA nests at different elevations and maintained in the lab under normal conditions (28±2°C, RH 55±5%). To test thermal adaptation at physiological and behavioral levels, two sets of chill coma recovery experiments were conducted including short-term (4°C for 30 minutes) and long-term (4°C for 15 hours), where LCA workers from each nest were divided into two groups with one exposed to 4°C for 30 minutes and the other one to 4°C for 15 hours, followed by dislocation to normal conditions for recovery. Noted that both experiments were carried out for the LCA workers within three

NOTE

days after the nests were collected to avoid artifacts associated with prolonged acclimation period under laboratory conditions. Recovery patterns of 30 LCA foragers per nest from both experimental settings were recorded: in short-term treatment time required for all foragers recovering was recorded, while in long-term treatment we recorded the number of recovering foragers every 30 minutes as well as accumulated mortality. For both treatments, behavior of antenna cleaning serves as an index to define recovery of individual ant from frozen stupor. Significance of recovery patterns was tested using Welch ANOVA and Games-Howell test for short-term treatment but not long term one as the number of workers is insufficient to complete at least three replicates in the latter one. Hence, we observed the trend of the recovery patterns for the long term treatment only.

Results and discussion

Results of short-term chill coma recovery revealed a negligible correlation between recovery time and elevations as considerable variations of recovery time are observed among individuals from different populations (Fig. 2). In long-term treatment, however, most of individuals from nests collected from mid-high elevations generally are characterized by faster recovery time as well as lower mortality compared to those from lowland (Fig. 3), suggesting that cold tolerance likely have been developed and operated during colonization into mid-high elevations by LCA. Nevertheless, results presented here are based on a limited number of LCA nests; greater sample size therefore is required to test if such trend remains significant.

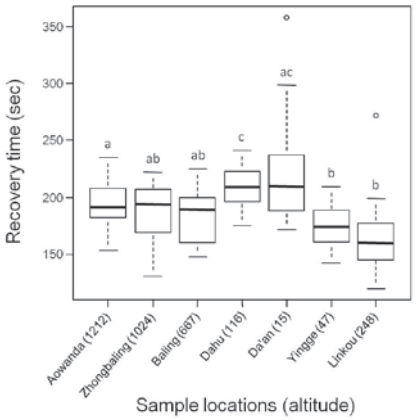

Figure 2. The recovery time of LCA workers after short-term cold treatment. Box-plots with the same letter are not significantly different. Open circles denote outlier data point.

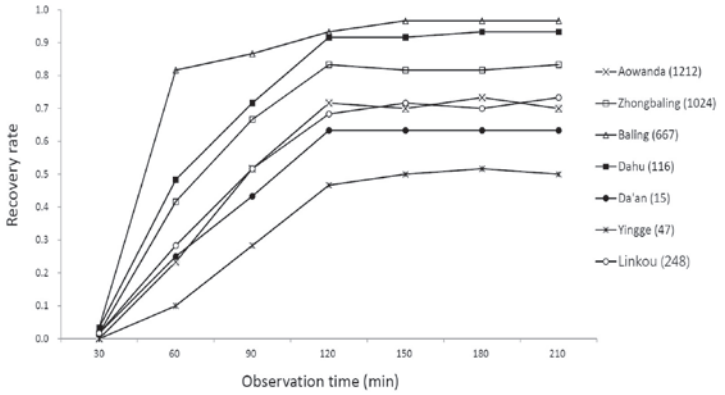

Figure 3. The recovery rate and accumulated mortality of LCA workers after long-term cold treatment (accumulated mortality = 1- recovery rate).

Outlook on future research

It is believed that LCA was introduced into Japan in early 20th century (with the earliest known record dated back to 1924) and have spread across entire Okinawa Islands and southern Kyushu area (ex. Kagoshima Prefecture) since then [2]. In addition, populations of LCA can be found sporadically in other areas of mainland Japan where appear to be non-preferable environment for LCA especially during the winter. Together with the finding of successful colonization of LCA into mid-high elevation in Taiwan, LCA serves as a rare yet excellent system to understand how invasive ants of tropical origin overcome environmental stresses at both high latitude and altitude.

My laboratory therefore aims to use a multidisciplinary approach combining genetics, genomics, physiology and behavior to study the mechanisms underlying latitudinal and altitudinal adaptation of LCA. Firstly, extensive survey is expected to conduct in Kagoshima Prefecture, and distribution of LCA will be accordingly mapped out. Genetic markers are developed and subsequently employed to confirm long-term population persistence for LCA using pedigree/kinship analyses. Cold tolerance, chill coma recovery and

NOTE

supercooling point are assayed to understand if such adaptive potential results from behavioral or physiological plasticity. If such plasticity exists, we attempt to pinpoint the genomic region associated with thermal regulation by mining the functional genomic database that was previously established. Results are expected to serve as baseline information for development of management strategy on ant invasion under different temperature regimes. Several collaborators are included in this study: Tsuyoshi Yoshimura at RISH, Chow-Yang Lee at Universiti Sains Malaysia, Alexander Mikheyev at Okinawa Institute of Science and Technology and DeWayne Shoemaker at University of Tennessee at Knoxville.

References

[1] Wetterer J. 2015. Geographic origin and spread of cosmopolitan ants (Hymenoptera: Formicidae). *Halteres* 6: 66-78.

[2] Wetterer J. 2008. Worldwide spread of the longhorn crazy ant, *Paratrechina longicornis* (Hymenoptera: Formicidae). *Myrmecological News* 11: 137-149.

RECENT RESEARCH ACTIVITIES

Non-destructive technique for wood identification

(Laboratory of Biomass Morphogenesis and Information, RISH, Kyoto University)

Junji Sugiyama, Kayoko Kobayashi, and Suyako Tazuru

Our resent interests are to establish non-destructive testing methods to evaluate a variety of information from a given wood specimen, such as species, tree-rings, anatomical features, chemical composition, and physical properties. Among them, novel wood identification techniques developed recently, by making full use of wood database maintained at Xylarium, will be outlined briefly.

Near Infrared spectroscopy and multivariate analyisis

Near-infrared (NIR) spectroscopy, which is known as a rapid, accurate and reproducible technique, is an attractive choice. NIR spectroscopy is also suitable for assessing wood materials because the bands attributable to the vibrations of the chemical bonds involved in the formation of the cell wall allow for the direct and indirect estimation of the chemical and physical properties of the materials. When combined with multivariate analysis, NIR spectroscopy has potential to distinguish even species.

Pinus densiflora and *P. thunbergii* are varieties of pine trees that are very popular in Japan. The former is known as akamatsu, and the latter as kuromatsu. Both habitats are disributed widely in Japan. *P. densiflora* is commonly seen growing on the low mountains and hill- sides, while *P. thunbergii* is native to the coastal areas. Anatomically, these two species are nearly identical except for the degree of dentate thickening of the ray tracheids. When analysing present heartwood samples, NIR gave nearly perfect ability of correct identification [1]. Similar study is extended to investigate Korean pine wood used in traditional buildings, which showed that *P. densiflora*, and *P. sylvestris* were distinguishable [2,3].

However, when aging wood samples were used, the proposed discriminant function was found to be ineffective. Therefore, identification of aged wood samples from historical buildings by NIR is still questionable and requires more analysis to separate species-specific information from aging effect in the spectra [1].

Image recognition by texture analyisis

Kyushu National Museum was the fourth national museum in Japan, and it is devoted to the scientific investigation of artwork. Since the installation of a large-scale X-ray CT instrument, nearly 2000 wooden artifacts have been inspected. Unfortunately, the images were never considered as resources for analyzing wood properties. This is because the resolution of the image was too low to apply conventional wood identification that relies on the visual inspection of microscopic anatomical features. However, inspired by the recent advance in machine learning, the computer-aided recognition of low-resolution CT images recorded at Kyushu National Museum seemed to have a potential to be uncovered.

Recently, we constructed a original system for wood identification from low-resolution CT data using the GLCM and k-NN algorithm as a feature extractor and classifier, respectively. The system recognized 10 representative wood samples for sculpture almost perfectly, and the system is under continuous improvement [4].

References

[1] Horikawa Y, Mizuno-Tazuru S, Sugiyama J, “Near-infrared spectroscopy as a potential method for identification of anatomically similar Japanese diploxylons”. *J Wood Sci* vol. 61, 251-261, 2015.

[2] Hwang SW, Lee WH, Horikawa Y, Sugiyama J, “Chemometrics approach for species identification of *Pinus densiflora* Sieb. et Zucc. and *Pinus densiflora* for. *erecta* Uyeki (in Korean)”, *J Kor Wood Sci Technol*, 43, 6, 701-713, 2015.

[3] Hwang SW, Lee WH, Horikawa Y, Sugiyama J, “Identification of *Pinus* species related to historic architecture in Korea by using NIR chemometric approaches”, *Journal of Wood Science*, vol. 62, 156-167, 2016.

[4] Kobayashi K, Akada,M, Torigoe T, Imazu S, Sugiyama J “Automated recognition of wood used in traditional Japanese sculptures by texture analysis of their low-resolution computed tomography data”, J Wood Sci. vol. 61, 630-640, 2015.

RECENT RESEARCH ACTIVITIES

Use of biphenyl/polychlorinated biphenyl-degrading bacteria for the production of useful aromatic compounds

(Laboratory of Biomass Conversion, RISH, Kyoto University)

Takahito Watanabe, Hidehiko Fujihara, Jun Hirose, Hikaru Suenaga, and Nobutada Kimura

Most of aromatic compounds sourced from nature are derived from plant lignin. Lignin is a recalcitrant aromatic heteropolymer; however, some species of basidiomycetes, collectively known as white-rot fungi, can degrade lignin in wood. When these fungi partially degrade lignin, many of its degradation products, containing lignin-derived aromatic compounds, are released into natural environments. Especially, in soil environments, there are a large number of bacteria grown on lignin-derived aromatic compounds.

On the other hand, so far we have isolated 14 biphenyl-utilizing/degrading bacteria, belonging to the genera *Pseudomonas* and *Rhodococcus*, from various environmental samples. Because these bacteria can also co-metabolically degrade polychlorinated biphenyls (PCBs), xenobiotic compounds known as one of the most serious environmental pollutants, we have extensively studied on biochemical and genetic bases of biphenyl/PCB degradation [1]. Furthermore, we have recently performed the whole genome sequencing of these biphenyl/PCB-degrading bacteria and compared their genomes with those of other xenobiotic compound-degrading bacteria [2-10]. Interestingly, the genome analyses revealed that these biphenyl/PCB-degrading bacteria possess various catabolic genes involved in the degradation of lignin-derived aromatic compounds, as well as xenobiotic aromatic compounds. In fact, some of the sequenced bacteria were able to grow well on lignin-derived aromatic compounds as the sole sources of carbon and energy. These findings show that many aromatic compound-catabolic genes may be functionally expressed in the presence of lignin-derived aromatic compounds.

In this study, we focus on the production of useful aromatic compounds from wood biomass, such as lignin-derived aromatic compounds, by molecular breeding of aromatic compound-catabolic genes from the biphenyl/PCB-degrading bacteria. We are now trying to screen and identify useful genes and proteins from these bacteria using genomics and proteomics technologies.

References

[1] Furukawa, K., and Fujihara, H., *J. Biosci. Bioeng*., 105, 433-449, 2008.

[2] Kimura, N., *et al*., *Genome Announc*., 3(2):e00059-15. doi:10.1128/genomeA.00059-15, 2015.

[3] Suenaga, H., *et al*., *Genome Announc*., 3(2):e00142-15. doi:10.1128/genomeA.00142-15, 2015.

[4] Suenaga, H., *et al*., *Genome Announc*., 3(2):e00143-15. doi:10.1128/genomeA.00143-15, 2015.

[5] Watanabe, T., *et al*., *Genome Announc*., 3(2):e00222-15. doi:10.1128/genomeA.00222-15, 2015.

[6] Watanabe, T., *et al*., *Genome Announc*., 3(2):e00223-15. doi:10.1128/genomeA.00223-15, 2015.

[7] Fujihara, H., *et al*., *Genome Announc*., 3(3):e00473-15. doi:10.1128/genomeA.00473-15, 2015.

[8] Fujihara, H., *et al*., *Genome Announc*., 3(3):e00517-15. doi:10.1128/genomeA.00517-15, 2015.

[9] Hirose, J., *et al*., *Genome Announc*., 3(5):e01214-15. doi:10.1128/genomeA.01214-15, 2015.

[10] Hirose, J., *et al*., *Genome Announc*., 3(5):e01215-15. doi:10.1128/genomeA.01215-15, 2015.

RECENT RESEARCH ACTIVITIES

Studies on Structure, Biosynthesis, and Biongineering of Lignocellulose and Phenylpropanoid Metabolites

(Laboratory of Metabolic Science of Forest Plants and Microorganisms, RISH, Kyoto University)

Toshiaki Umezawa, Yuki Tobimatsu, Shiro Suzuki, and Masaomi Yamamura

It is becoming increasingly important to establish a sustainable society that depends on renewable resources. As lignocellulosic biomass is the most abundant renewable and carbon-neutral resource on earth, technologies to improve their productivity and utilization properties are key for realizing the goal. In this context, we investigate structure, biosynthesis and bioengineering of lignocellulosic biomass produced in various model plants and biomass crops. In addition, we are interested in understanding biosynthetic mechanism of phenylpropanoid dimers that show various useful biological activities. Our program typically integrates many research ideas and approaches based on organic chemistry, biochemistry, and molecular biology.

Among a wide variety of biomass feedstocks, large-sized grass species have attracted particular attention especially because of their superior biomass productivity. We therefore have been interested in understanding structure and properties of biomass produced in a variety of large-sized grass species. We recently elucidated chemical structures as well as enzymatic saccharification efficiency of biomass produced in different tissues isolated from *Erianthus*, *Sorghum*, and sugarcane, and demonstrated that structure and assembly of cell wall lignin considerably vary among the tissues and species, and substantially impact the conversion of biomass to bioethanol [1,2].

We are also interested in metabolic engineering of grass lignocelluloses to improve their production and utilization properties; for this research purpose, we use rice as a model plant. In particular, our research focuses on lignin, a key component of lignocellulosic biomass. We together with collaborators have characterized various rice transgenic and mutant lines in which specific genes encoding enzymes and transcription factors in the lignin biosynthetic pathway were down- and/or up-regulated. Until now, we have identified several transgenic/mutant lines displaying intriguing lignin phenotypes, which are potentially useful for enhanced biomass utilizations [3-6].

Aiming at biological production of plant phenylpropanoid dimers including lignan and norlignan, we have been characterizing enzymes/genes involved in the formation of such compounds. In addition, we are also examining their conversion in mammals. Our recent projects include identification of genes involved in the biosynthesis of an antitumor lignan, podophyllotoxin, unravelling crystal structures of an enzyme involved in norlignan biosynthesis, (*Z*)-hinokiresinol synthase, and identification of demethylase involved in enterolignan biosynthesis in a human intestinal bacterium [7].

References

[1] Miyamoto T, Yamamura M, Tobimatsu Y, Suzuki S, Kojima M, Takabe K, Umezawa T (2016) Abstracts of the 66th Annual meeting of the Japan Wood Research Society, p. 148.

[2] Hayashi A, Yamamura M, Tobimatsu Y, Miyamoto T, Kojima M, Takabe K, Suzuki S, Umezawa T (2016) Abstracts of the 66th Annual meeting of the Japan Wood Research Society, p. 150.

[3] Takeda Y, Koshiba T, Tobimatsu Y, Hattori T, Sakamoto M, Takano T, Suzuki S, Umezawa T (2015) Proceedings of the 60th Lignin Symposium, Tsukuba, Japan, p. 112-115.

[4] Lam PY, Tobimatsu Y, Zhu F-Y., Chan WL, Liu H, Umezawa T, Lo C. T (2016) Abstracts of the 66th Annual meeting of the Japan Wood Research Society, p. 115.

[5] Matsumoto N, Takeda Y, Tobimatsu Y, Koshiba T, Suzuki S, Sakamoto M, Umezawa T (2016) Abstracts of the 66th Annual meeting of the Japan Wood Research Society, p. 223.

[6] Takeda Y, Koshiba T, Tobimatsu Y, Murakami S, Yamamura M, Sakamoto M, Suzuki S, Umezawa T (2016) Abstracts of the 66th Annual meeting of the Japan Wood Research Society, p. 114.

[7] Kawamura A, Suzuki A, Yoneda Y, Nishida T, Kawai S, Yamamura M, Suzuki S, Umezawa T (2015) Abstracts of the 33th Annual meeting of the Japanese Society for Plant Cell and Molecular Biology, p. 134.

RECENT RESEARCH ACTIVITIES

Differential effects of caffeine on phytopathogenic and mycoparasitic fungal growth

(Laboratory of Plant Gene Expression, RISH, Kyoto University)

Akifumi Sugiyama and Kazufumi Yazaki

Biological roles of secondary metabolites in rhizosphere were proposed to plant growth regulation, plant-microbe interactions, function in nutrient acquisition, and regulation of microbial community structure. Regarding the interaction with microbes, root exudates serve as signaling molecules, inhibitors and repellants. One of the most popular secondary metabolite is caffeine (1,3,7-trimethylxanthine), which is produced in coffee and tea plants. The physiological functions of caffeine in plants have been proposed to restrict development and growth of other organisms, which is often referred to as allelopathy. Caffeine also indirectly stimulates plant defense response, which is referred to as priming.

Coffee roots secrete caffeine into the culture medium, resulting in an average concentration of 0.03%. Tea seedlings also secrete caffeine up to 0.05% a day.Caffeine released from the primary root was suggested to help seedlings to establish the rhizosphere microbial and physical environment, which was partially substantiated by the finding that coffee rhizosphere was rich in particular fungal species, Trichoderma. Many of *Tricoderma* have been known to kill other fungi. This phenomenon is called mycoparasitism and applied to biocontrol in agriculture. In this study, the effect of caffeine on filamentous fungi, both Trichoderma species and pathogens, were examined.

Eight fungal species were cultured on potato dextrose agar plates with or without caffeine. *Rhizoctonia solani* grew 17 mm/day and 8 mm/day in the absence and the presence of caffeine, respectively. *Fusarium oxysporum* and *Sclerotinia sclerotiorum* grew slower than *R. solani*I Inhibition in growth by caffeine varied depending on species with the growth velocity in the presence of caffeine was about 3 mm/day for pathogens and 7.5 mm/day for *Trichoderma*. The finding showed that the inhibitory efficiency of caffeine is differential, i.e. caffeine may favor predators when they co-grown with prey fungi. Interaction between the prey and the predator was also studied with confrontation test. In the control plate without caffeine, the prey (*F. oxysporum*) steadily grew after inoculation, while in the plate with caffeine, it also grew with reduced velocity. When the prey was co-cultured with the predator (*T. virens*) without caffeine, contact occurred at day 4. When the prey was co-cultured with *T. virens* in the with caffeine, contact occurred before day 7. In both cases, upon contact, growth of the *F. oxysporum* ceased, whereas that of *T. virens* continued, indicating an active mycoparasitism to have occurred.

In summary, these results together with the previous publications suggest that 1) caffeine functions as allelopathic defense by directly suppressing the growth of pathogen, 2) caffeine attracts *Trichoderma* to cope with pathogens, 3) *Trichoderma* allies with coffee plants to secure nutrients and environment, 4) interaction between coffee and *Trichoderma* is mutually beneficial and caffeine fosters the connection. In this regard, caffeine functions as a powerful weapon in arms race between coffee plants and pathogens by fostering enemy's enemy. This phenomenon could be regarded as the previously unidentified role of caffeine, and be called "caffeine alliance".

Reference

A. Sugiyama, C.M. Sano, K. Yazaki, H. Sano, "Caffeine fostering of mycoparasitic fungi against phytopathogens" Plant signaling & behavior 11 (1), e1113362, 2016.

RECENT RESEARCH ACTIVITIES

RASS (Radio Acoustic Sounding System): A new radar observation technique for profiling atmospheric temperature

(Laboratory of Atmospheric Sensing and Diagnosis, RISH, Kyoto University)

Toshitaka Tsuda

The operational weather station of a meteorological agency normally employs a balloon-borne radiosonde to measure temperature (T) profiles. However, the temporal resolution of radiosondes is 12-24 hr, which is insufficient to investigate details of the medium (meso)-scale meteorological phenomena such as the cumulonimbus convection accompanying a severe rain event with time scales of a few hours in their generation and development processes. Radio Acoustic Sounding System (RASS) has been developed as a radar remote-sensing technique to continuously observe atmospheric temperature profiles. RASS consists of a wind profiling radar (WPR), such as the MU radar, Equatorial Atmosphere Radar (EAR), and a boundary layer radar (BLR), and an acoustic transmission system. Figure 1 shows the basic principle of RASS. A large power sound is emitted high up into the sky, then, refractive index (n) variations are artificially created associated with the upward propagation of the sound waves. WPR can detect faint radio wave scattering by the n perturbations, which is called the RASS echo. The speed of sound (C_s) is measured from the Doppler frequency shifts of the RASS echo. Then, we can determine a T profile using a relationship that C_s is proportional to $\sqrt{T}$.

When RASS is applied to WPR operated on the 50 MHz band, like the MU radar and EAR, we use sound waves with a frequency of about 100 Hz, considering the Bragg condition for obtaining strong RASS echoes. Because such low frequency sound can propagate up to high altitudes without suffering dissipation due to atmospheric turbulence, RASS with the MU radar was able to measure T profiles up to 23 km under an ideal condition, exceeding the tropopause at 10-15 km altitude. The accuracy of T with RASS was about 0.2 K in comparison to simultaneous radiosonde results.

RASS is also applied to BLR that is designed to measure the lowest part of the atmosphere from 100 m to several kilometers in altitude. Figure 2 shows the time variations of T observed by RASS with BLR at PUSPIPTEK, Serpong, near Jakarta in Indonesia, showing a clear diurnal variation of T due to heating of the surface by the solar radiation. RASS can visualize time and height variations of the temperature associated with meso-scale meteorological phenomena, and it is also useful to observe transport and mixing of minor atmospheric constituents and aerosol particles.

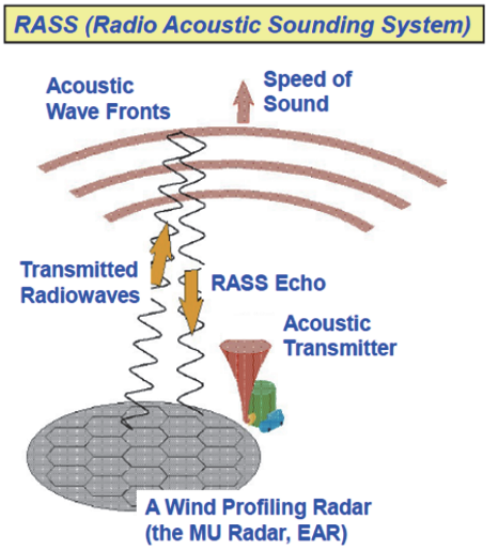

Figure 1. Basic concept of RASS

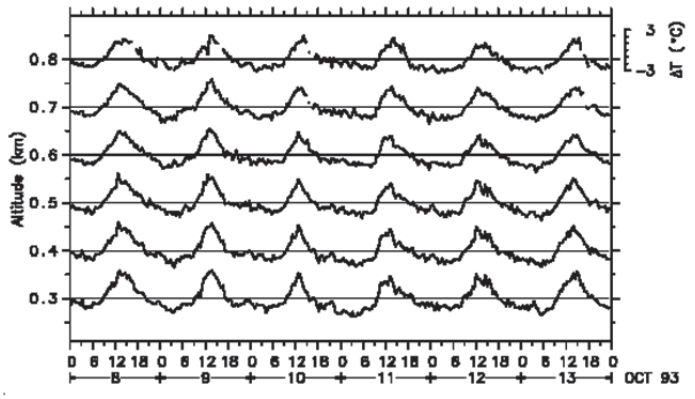

Figure 2. Time variations of temperature perturbations at 0.3-0.8km altitude, observed with a BLR-RASS (1357.5 MHz, peak power=1 kW) on October 8-13, 1993. Original time resolution is 3 min., but, results are averaged for 30 min. Difference from simultaneous radiosonde soundings was within 0.5 K. Amplitude of 24-hour oscillation was 1.8 K with maximum at 14 LT.

RECENT RESEARCH ACTIVITIES

Mesospheric ozone variations during the solar eclipse

(Laboratory of Atmospheric Environmental Information Analysis, RISH, Kyoto University)

Kenshi Takahashi and Masato Shiotani

Atmospheric ozone (O_3) plays an important role in determining the thermal and dynamical structure of the middle atmosphere through radiative and chemical processes. To monitor the global distribution of O_3 and related trace gases, the Superconducting Submillimeter-Wave Limb-Emission Sounder (SMILES) was developed and deployed on the Japanese Experiment Module (JEM) of the International Space Station (ISS) [1]. The SMILES successfully observed vertical distributions of O_3 concentration in the middle atmosphere during the annular solar eclipse that occurred on 15 January 2010. In the mesosphere, where the photochemical lifetime of O_3 is relatively short (ca. 100 s), altitude-dependent changes in O_3 concentration under reduced solar radiation and their temporal variations were clearly observed as a function of the eclipse obscuration (Figure 1). This study reported for the first time the vertical distributions of mesospheric O_3 during a solar eclipse event, and analyzed theoretically the eclipse-induced changes. Full text of this report will be found in the journal article [2]. We showed that simple analytical expressions describing the daytime O_3 concentration under photochemical steady state approximations can be used to analyze the eclipse-induced changes in O_3 concentration, providing a unique opportunity to verify our current knowledge of the key chemical processes involving odd oxygen and HO_x radicals in the daytime mesosphere. Hitherto, testing our understanding of the mesospheric photochemistry mostly involved evaluating the consistency of day-to-night variations in O_3 and HO_x concentrations between the observations and model calculations. This study has highlighted that highly sensitive, altitude-resolved measurements of mesospheric O_3 under reduced solar radiation can provide valuable data to test our understanding of the chemical processes in the daytime mesosphere.

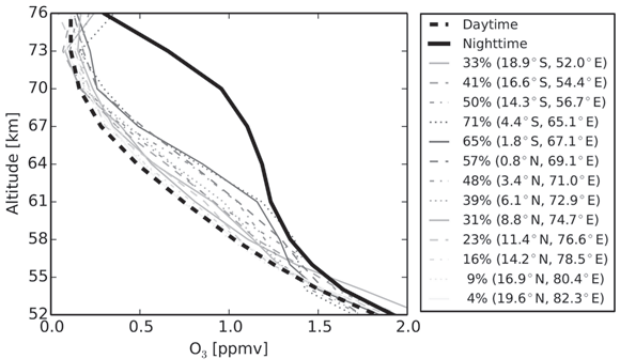

Figure 1. Vertical profiles of O_3 during the eclipse. Profile location and corresponding eclipse obscuration are shown in the legend; the dashed lines are for the southern part of the eclipse center. The black solid and dashed lines are the mean daytime and nighttime profiles of O_3 concentration, respectively. (Courtesy of Dr. Koji Imai)

Acknowledgements

This was a collaborative research between Japan Aerospace Exploration Agency, National Institute for Environmental Studies and RISH.

References

[1] Kikuchi, K., Nishibori, T., Ochiai, S., Ozeki, H., Irimajiri, Y., Kasai, Y., Koike, M., Manabe, T., Mizukoshi, K., Murayama, Y., Nagahama, T., Sano, T., Sato, R., Seta, M., Takahashi, C., Takayanagi, M., Masuko, H., Inatani, J., Suzuki, M., Shiotani, M. (2010), "Overview and early results of the Superconducting Submillimeter-Wave Limb-Emission Sounder (SMILES)", *J. Geophys. Res.*, 115, D23306, doi:10.1029/2010JD014379.

[2] Imai, K., Imamura, T., Takahashi, K., Akiyoshi, H., Yamashita, Y., Suzuki, M., Ebisawa, K. and Shiotani, M. (2015), "SMILES observations of mesospheric ozone during the solar eclipse", *Geophys. Res. Lett.*, 42, doi:10.1002/2015GL063323.

RECENT RESEARCH ACTIVITIES

Shigaraki UAV-Radar Experiment (ShUREX)

(Laboratory of Radar Atmospheric Science, RISH, Kyoto University)

Hiroyuki Hashiguchi and Mamoru Yamamoto

The Shigaraki UAV-Radar Experiment (ShUREX) is an international US-Japan-France observation field campaign (PI: Prof. L. Kantha of University of Colorado), aimed at measuring and obtaining a better understanding of turbulent mixing and structures in the lower atmosphere. ShUREX 2015 and 2016 campaigns were carried out at the Shigaraki MU Observatory in June 1-14, 2015 and May 26-June 13, 2016, respectively. During the campaign, the unmanned aerial vehicle (UAV) DataHawk, which was developed at the University of Colorado, Boulder, and equipped with a high-resolution cold wire and a high-resolution pitot tube, along with an IMET sonde, was flown near and over the MU radar to obtain simultaneous measurements of the atmospheric column over the radar. It enabled the comparison of radar-inferred refractive index structure function parameter C_n^2 with that obtained from measurements by the cold wire and the humidity sensor on the UAV. It also permitted comparison of TKE dissipation rates in the turbulent structures inferred from the radar spectral broadening with those measured directly by the UAV velocity sensor.

Figure 1 shows the DataHawk UAV which has been developed at the University of Colorado. The wingspan and mass are about 1 m and 1 kg, respectively. It is propelled by a pusher prop in the rear powered by an electric motor running on LiPo batteries. It could be catapult (bungee-cord) launched or taken aloft by a standard meteorological balloon and deployed from a height to conserve battery power. It has an endurance of 60-90 minutes depending on the climb rate. Airspeed ranges from 10 to 25 m/s. The UAV equipped with autopilots can be pre-programmed to execute a preplanned trajectory, and the sensors on board can make atmospheric measurements (pressure, temperature, winds, etc.) along the trajectory. This trajectory can be a spiraling ascent and descent to a prescribed altitude over a particular spot. It can also be a racetrack type trajectory. The range is around 20 to 40 km, determined by the uplink/downlink antenna gain. The DataHawk is well suited to making atmospheric measurements up to altitudes of 4 km (bungee launch) and 7 km (balloon launch). It uses GPS for navigation. The design of the DataHawk, the characteristics of ground support components and some data collected from these systems are described by Lawrence and Balsley (2013) and Balsley et al. (2013). High-resolution (100 Hz) velocity and temperature sensors, capable of yielding information on turbulence, in addition to mean quantities can be deployed.

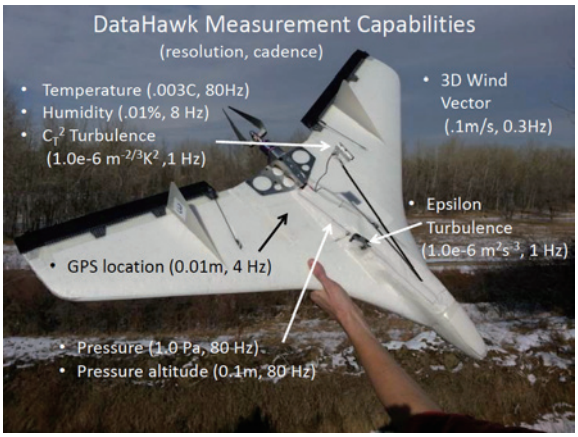

Figure 1. UAV developed by the University of Colorado. [Lawrence and Balsley, 2013]

References

[1] D. A. Lawrence and B. B. Balsley, High-resolution atmospheric sensing of multiple atmospheric variables using the DataHawk small airborne measurement system, *J. Atmos. Oceanic Technol.*, **30**, 2352-2366, 2013.

[2] B. B. Balsley, D. A. Lawrence, R. F. Woodman, and D. C. Fritts, Fine-scale characteristics of temperature, wind, and turbulence in the lower atmosphere (0-1,300 m) over the south Peruvian coast, *Bound.-Layer Meteor.*, **147**, 165-178, 2013.

RECENT RESEARCH ACTIVITIES

"Japan-USA Invasive Ant Consortium" formed to study invasive ants originated from Japan

(Laboratory of Ecosystem Management and Conservation Ecology, RISH, Kyoto University)

Chin-Cheng Yang

Recently I was invited to join the ''Japan-US Invasive Ant Consortium'' led by Prof. Tsuji at Ryukyu University in which various ant species invading into the US from Japan will be studied through implementation of multidisciplinary approaches. North Carolina State University serves as the main collaborating organization from the US side, whereas numerous Japanese research groups were involved in this consortium including those from Ryukyu University, Kyoto University (Prof. Matsuura and myself) and Kyoto Institute of Technology (Prof. Akino). Here is a brief summary of the missions and objectives of this international consortium as described below.

Numerous ant species originating from Japan have invaded into US: a project description

A total of four species have been found introduced into United States including *Tetramorium tsushimae, Nylanderia flavipes, Vollenhovia emeryi* and *Brachyponera chinensis* (Fig. 1) in last two decades presumably due to increasing international trade and anthropogenic activity. The four species were shown to impose significant negative impacts on the forest ecosystem, native biodiversity and urban sustainability [1].

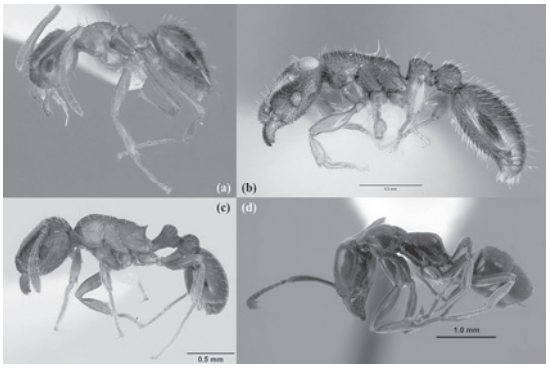

Figure 1. Ant species introduced into United States from Japan, including (a) *Nylanderia flavipes*, (b) *Vollenhovia emeryi*, (c) *Tetramorium tsushimae* and (d) *Brachyponera chinensis*. Note the scale bars are not standardized due to formatting purpose.

The consortium offers a real-time mutual resource-sharing platform where research outcomes of the targeted ants in both their home and introduced ranges will be distributed to all members for facilitation of research progress in each group of the consortium. Research topics are mainly directed towards those key traits that potentially make them invasive, which include genetics, behavior and colony structure. Ecological impacts such as reduction of local fauna also will be quantified, and, from an applied perspective, parasite/pathogen survey will be carried out for exploitation of potential biological control agents. Conclusively speaking, this project not only aims to understand factors associated with invasion success of these ants through comparative studies, but also eagers to learn the impacts of these ants as well as to evaluate feasibility of developing self-sustaining control measures. My lab will be focused on genetics (developing genetic resources and assessment of population genetic structure in both ranges) and microbial survey (mostly virus and *Wolbachia*), with an ultimate goal of characterization of genetic changes during invasion and microbial-based biocontrol scheme for these invasive pest ants.

Acknowledgements

I am sincerely grateful to Prof. Tsuji at Ryukyu University and Prof. Matsuura at Kyoto University for inviting me to join the consortium, and thanks also go to members of the consortium including Dr. Dobata, Dr. Kobayashi (Kyoto University), Prof. Akino (Kyoto Institute of Technology) and Dr. Clint (North Carolina State University) for welcoming me in this consortium.

Reference

[1] Wetterer J. 2015. Geographic origin and spread of cosmopolitan ants (Hymenoptera: Formicidae). *Halteres* 6: 66-78.

RECENT RESEARCH ACTIVITIES

Preparation of a high concentration cellulose nanofiber

(Laboratory of Active Bio-based Materials, RISH, Kyoto University)

Kentaro Abe and Hiroyuki Yano

The drying process in typical pulp production generates strong hydrogen bonding between cellulose microfibrils in refined cell walls and increases the difficulty in obtaining uniform cellulose nanofibers. In this study, we applied a ball-milling method in NaOH solutions to prepare a high-concentration cellulose nanofibers from dried pulp. NaOH treatments loosened the hydrogen bonding between cellulose microfibrils in dried pulps [1].

A dried bleached kraft pulp from softwood with an α-cellulose content of 90% was used. 8 wt% pulps immersed in 8% (w/w) NaOH aqueous solutions at room temperature. Nanofibrillation of pulps was performed using a ball mill (TSG-6U, IMEX Co. Ltd., Sooka, Japan) at 2000 rpm for 90 min with 5-mm zirconia balls at a filling rate of 33% (v/v). The samples were separated from the beads by filtration.

After fibrillation by ball milling in 8% NaOH solution for 90 min, smooth suspensions were obtained for all samples (Figure 1). FE-SEM observation revealed that fine nanofibers with a uniform diameter of approximately 12–20 nm were formed (Figure 2). These nanofibers are comparable to those prepared from never-dried refined wood samples using a grinder [2]. This result suggests that 8% NaOH treatment disrupted the hydrogen bonds between microfibrils in dried pulps and improved their nanofibrillation.

Interestingly, the nanofiber suspensions prepared in 8% NaOH were formed into hydrogels by neutralization because of surface entanglement and/or interdigitation between the nanofibers [3, 4]. Therefore, our method did not allow preparation of individual cellulose nanofibers in water from dried pulps. However, we are currently applying this method to the direct preparation of high-strength cast films and spun fibers. For general preparation of cellulose-based films and spun fibers, cellulosic raw materials must be dissolved using specific chemical agents such as carbon disulfide for rayon and cellophane. In contrast, our method can introduce formability to dried pulps without any dissolution process. In particular, nanofibrillation in 8 % NaOH solution can produce free-form cellulosic products while maintaining the original cellulose I crystal form, which has higher elastic modulus than cellulose II (cellulose I: 138 GPa, cellulose II: 88 GPa). Consequently, high-strength cellulosic products such as films and fibers can be produced with relative safety using only NaOH and coagulants.

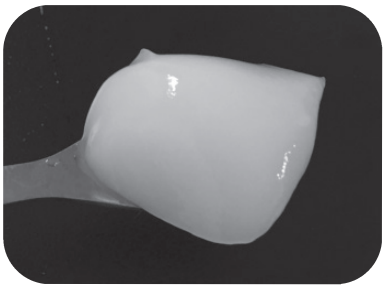

Figure 1. Appearance of 8 % cellulose nanofiber suspension in 8 % NaOH solution.

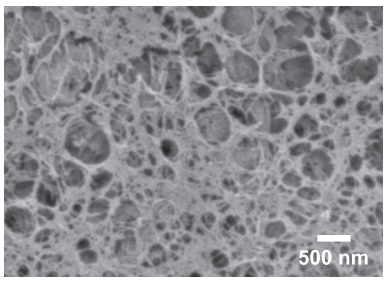

Figure 2.FE-SEM micrograph of freeze-dried cellulose nanofiber.

References

[1] Abe K, *Cellulose*, **23**, 1257-1261, 2016.

[2] Abe K, Iwamoto S, Yano H. *Biomacromolecules*. **8**: 3276-3278, 2007.

[3] Abe K, Yano H. *Carbohydrate Polymers.* **85**: 733-737, 2011.

[4] Abe K, Yano H. *Cellulose*. **19**: 1907-1912, 2012.

RECENT RESEARCH ACTIVITIES

Development of techniques for highly controlled chemical treatment in wood flow forming

(Laboratory of Sustainable Materials, RISH, Kyoto University)

Soichi Tanaka

Recently, chemical treatment techniques required for wood flow forming have been studied. In the wood flow forming process, the bulk wood is processed into the compact with a favorite form by being compressed and flowed into a mold. To obtain stable compact, the chemical substance is required to be introduced into cell walls in wood raw material before the forming process. The chemically treated compact, however, still had color change and roughness on surface, and its dimension was unstable (Figure 1). This may be caused by the presence of many cells that are not chemically treated (macroscopic irregularity) and of much unstable region in each cell wall (microscopic irregularity) in the compact. In my recent research, it has been noticed that fulfilling every cells with solution of chemical substance (Issue 1) and filling up unstable region in cell walls with chemical substance (Issue 2) are important for preventing macroscopic and microscopic irregularities, respectively.

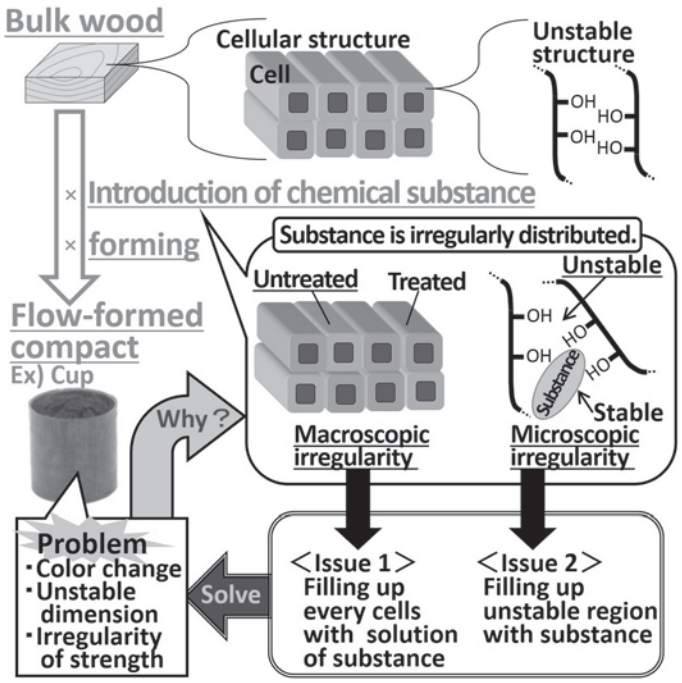

Figure 1. Issues in chemical treatment for wood flow forming.

Recent activity on Issue 1 is introduced here. One of the approach is to enhance the accessibility of solution to the inside of wood block. The representative method as such is to incise the block using edged tools, laser, *etc*. In the incising, however, the accessibility to the region except the wood surface is not so much enhanced. I noticed the wood block eaten by termites as a raw material of wood flow forming, because a lot of large holes are continued from the surface to the deep inside of the block, and because all the holes will disappear after flow forming process. The purpose of the study was to examine the effect of wood block eaten by termite on accessibility of chemical-substance-solution to the inside of the block. In the trial before the examination, the cup was flow-formed (Figure 2) using the block of pine eaten by Formosan subterranean termite (*Coptotermes formosanus*). Before the forming process, the eaten block was impregnated by a aqueous solution of phenol formaldehyde resin (50 wt%) and water was evaporated from it under an atmosphere at 20 °C and 32%RH. The compact was confirmed to be produced using termite-eaten-wood. As the next step, the amount of the chemical-substance-solution taken up by the wood block eaten by termite will be examined to confirm the feasibility of using this “termite-incising” technique as improving the accessibility of the solution to the inside of wood block.

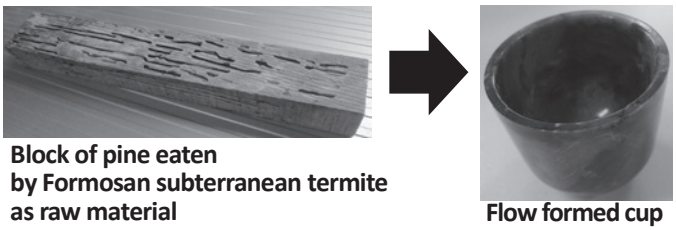

Figure 2. Raw material and flow formed compact.

Acknowledgements

I would like to express my gratitude to Dr. Yanagawa, Laboratory of Innovative Humano-Habitability, RISH, Kyoto University, for her giving me the wood block eaten by the termite.

RECENT RESEARCH ACTIVITIES

Development of Timber-Concrete Composite floor system using Glulam and CLT

(Laboratory of Structural Function, RISH, Kyoto University)

Takuro Mori, Akihisa Kitamori, and Hiroshi Isoda

1. INTRODUCTION

To decrease the building weight has an advantage in reducing the seismic force. Therefore it is considered that the reinforced-concrete (RC) and steel (S) structure partially using wooden material contributes to decrease the building weight. Our laboratory has focused on this research area. Last year, we showed a reinforce system for RC frame using CLT panel. In this year, we carried out a study on hybrid floor system of timber-concrete composite (TCC).

2. CONNECTION TEST

The glulam and CLT was employed as a beam and slab material respectively. The connection of wood materials and RC the steel plate was used to expect with high rigidity. The connection between wood materials and steel plate is glued by an adhesive, the connection between RC and steel plate is joined by an adhesion. The several type of connection between wood materials and RC were indicated high stiffness. Finally, composite floor experiments were carried out by using joint plates showed good results.

3. FULL SCALE TEST & DISCUSSIONS

Glulam beam type and CLT slab type experiment as composite floor system with RC slab was carried out for two and one specimens respectively (Fig1). The size of specimen was 2,000 x 6,000 mm, in span of 5,400 mm. As a result, the initial destruction occurred in all specimens by being peeled off along the glue line between wood and steel plate at around 100 kN load. Although initial destruction strength were not enough, it exhibited a high rigidity as expected (Fig2). The straight line as "plus both stiffness" in Fig2 was illustrated by simply adding stiffness of both the wooden materials and RC slab. Compared with the straight line and experimental curve, it was found the experimental stiffness increased from 2 to 2.5 times higher. In the future subject, we aim to use these TCC floor systems in practical application by improving initial destruction strength.

Fig1: Test scene of glulam beam with RC slab (Upper) and CLT with RC slab (Bottom)

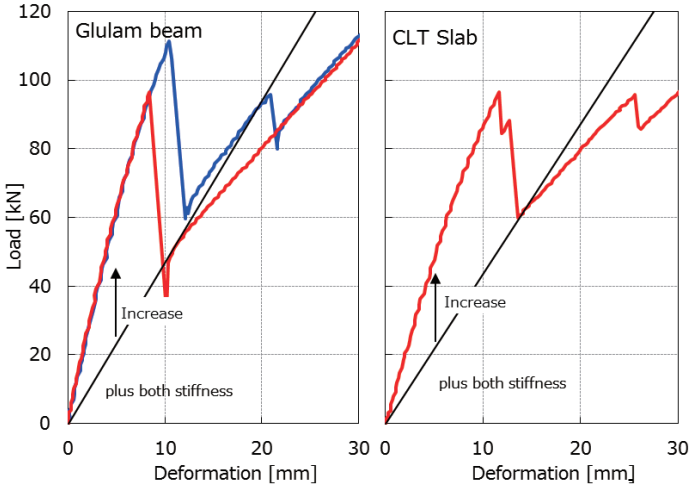

Fig2: Load-deformation curve comparison between experimental value and simply added both materials stiffness.

RECENT RESEARCH ACTIVITIES

Preparation and characterization of carbonized wood with metal ions for CO_2 capture

(Laboratory of Innovative Humano-habitability, RISH, Kyoto University)

Toshimitsu Hata

In view of global warming, the adsorption and separation of CO_2 gas are necessary to prevent the further increase of its concentration in the atmosphere. The use of fossil fuels has increased in recent times, and there is a growing interest in developing CO_2-gas adsorption materials for applications not only in industries but also in offices and homes[1)]. Till date, the amine absorption method, active carbon method, and molecular sieve method are the most popular, which are suitable for capturing CO_2 gas emitted from industries on a large scale[2)]. For example, the amine absorption method is used for collecting large-scale CO_2 emissions from thermal power stations. However, after use, a substantial amount of energy is required to collect the amine solution and it cannot be used repeatedly for a long time. On the contrary, the adsorption process using solid solvents for capturing CO_2 gas is suitable for middle- to small-scale CO_2 gas emissions. Its applicability depends on adsorption efficiency and cost. The development of a retention method for the low-cost and effective adsorption of CO_2 is urgently required.

CO_2 gas can more easily access micropores (at approximately 2 nm, at 100 kPa atmospheric pressure), compared to nitrogen, as the CO_2-saturated steam pressure is lower, approximately 3.48 MPa at 273 K. Therefore, obtaining a good separation from a gas mixture is possible. Low- cost and low-pressure capture of CO_2 gas can be achieved through the adsorption process using solid solvents.

Wood is a porous material and is composed of two types of pores: macropores and micropores. Micropores already exist in the cell walls of dry wood (Fig.1)[3)]. The authors reported that onion-like carbon structures grow during conventional carbonization on wood[4)]. The carbonization of such a material may provide better access for CO_2 gas to these micropores. In the present activity, solid adsorbents from raw Todo fir material are developed at a low cost, in comparison with conventional products, for effective CO_2 gas adsorption. Furthermore, high resolution transmission electron microscopy (HRTEM) is used to observe the micropores' texture to explain the adsorption mechanism.

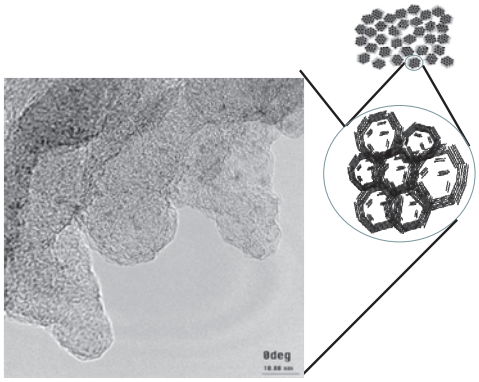

Fig.1 Formation of onion-like structures on wood obtained by heat treatment of wood[4)].

Acknowledgements

This work was supported by KAKENHI (16K05866), a Grant-in-Aid for Scientific Research (C) from the Japan Society for the Promotion of Science (JSPS); by the collaborative research of the Wood Composites Hall; and by the Analysis and Development System for Advanced Materials (ADAM) project of the Research Institute for Sustainable Humanosphere (RISH), Kyoto University.

References

1. http://www.jccca.org/
2. http://www.meti.go.jp/committee/kenkyukai/energy_environment/jisedai_karyoku/pdf/002_02_03.pdf
3. Kojiro, K.; Furuta, Y.; Ishimaru, Y., (2008) J. Wood Sci., 54 (3), 202-207.
4. Hata, T., et al. (2000). J. Wood Sci., 46 (1), 89-92.

RECENT RESEARCH ACTIVITIES

Simulations and Modeling of Geospace Environment

(Laboratory of Computer Space Science, RISH, Kyoto University)

Yoshiharu Omura and Yusuke Ebihara

Recent observations of plasmaspheric hiss emissions by the Van Allen Probes show that broadband hiss emissions in the plasmasphere comprise short-time coherent elements with rising and falling tone frequencies. Based on nonlinear wave growth theory of whistler mode chorus emissions, we have examined the applicability of the nonlinear theory to the coherent hiss emissions. We have generalized the derivation of the optimum wave amplitude for triggering rising tone chorus emissions to the cases of both rising and falling tone hiss elements. The amplitude profiles of the hiss emissions are well approximated by the optimum wave amplitudes for triggering rising or falling tones. Using the theory, we can infer properties of energetic electrons generating hiss emissions in the equatorial region of the plasmasphere.

We perform test particle simulations of energetic electrons interacting with whistler mode chorus emissions. We compute trajectories of a large number of electrons forming a delta function with the same energy and equatorial pitch angle. The electrons are launched at different locations along the magnetic field line and different timings with respect to a pair of chorus emissions generated at the magnetic equator. We follow the evolution of the delta function and obtain a distribution function in energy and equatorial pitch angle, which is a numerical Green's function for one cycle of chorus wave-particle interaction. By taking the convolution integral of the Green's functions with the distribution function of the injected electrons repeatedly, we follow a long-time evolution of the distribution function. We find the rapid formation of a dumbbell distribution of highly relativistic electrons within a few minutes after the onset of the continuous injection of 10–30 keV electrons.

Sudden brightening of aurora can be seen in the polar region at night. This phenomenon is called auroral breakup, and is a visible manifestation of a substorm. When the substorm takes place, the near-Earth space environment is severely disturbed. For example, energetic particles are injected into the near-Earth space, which can be a seed of radiation belt electrons. Large-scale current system is also developed, which can induce electric current in the power grid system on the ground. The substorm has been a challenging problem since the definition of a substorm was made in 1964. We utilized a global magnetohydrodynamics (MHD) simulation, and suggested the generation mechanism. The mechanism is quite different from previously suggested ones, but can explain many related phenomena reasonably (Figure 1) throughout the substorm from quiet time to substorm expansion [3][4][5]. Large-scale redistribution of the state of the magnetosphere and the magnetosphere-ionosphere coupling are found to be essential to cause the substorm.

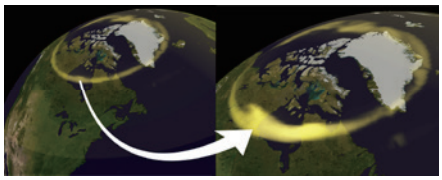

Figure 1. Simulated auroral breakup.

References

[1] Omura, Y., S. Nakamura, C. A. Kletzing, D. Summers, and M. Hikishima, Nonlinear wave growth theory of coherent hiss emissions in the plasmasphere, J. Geophys. Res. Space Physics, 120, 7642–7657, doi:10.1002/2015JA021520, 2015.

[2] Omura, Y., Y. Miyashita, M. Yoshikawa, D. Summers, M. Hikishima, Y. Ebihara, and Y. Kubota, Formation process of relativistic electron flux through interaction with chorus emissions in the Earth's inner magnetosphere, J. Geophys. Res. Space Physics, 120, 9545–9562, doi:10.1002/2015JA021563, 2015.

[3] Ebihara, Y., and T. Tanaka, Substorm simulation: Quiet and N-S arcs preceding auroral breakup, J. Geophys. Res., 121, doi:10.1002/2015JA021831, 2015.

[4] Ebihara, Y., and T. Tanaka, Substorm simulation: Formation of westward traveling surge, J. Geophys. Res., 120, doi:10.1002/2015JA021697, 2015.

[5] Ebihara, Y., and T. Tanaka, Substorm simulation: Insight into the mechanisms of initial brightening, J. Geophys. Res., 120, doi:10.1002/2015JA021516, 2015.

RECENT RESEARCH ACTIVITIES

Demonstration of Multicopter Assisted Wireless Batteryless Sensing System (WBLS)

(Laboratory of Applied Radio Engineering for Humanosphere, RISH, Kyoto University)

Naoki Shinohara, Tomohiko Mitani, Yohei Ishikawa, Junji Miyakoshi, and Shin Koyama

A wireless sensor application by using a flying drone is proposed by Kyoto University in 2015. One of weak point of the WPT is a miss match between a required power and system size of the WPT which includes an antenna size and a transmitting radio wave power. When a distance between a transmitting antenna and a receiving antenna of the WPT becomes longer, beam efficiency becomes lower than a user expectation. Even for the WPT sensor, it sometimes happens. By using the flying drone, the distance between a transmitting antenna and a receiving antenna of the WPT becomes shorter and WPT system can be smaller than that without the drone. The proposed WPT system is named a "Multicopter Assisted Wireless Batteryless Sensing System (WBLS)". The first experiment was carried out on July, 2015 at Advanced Microwave Energy Transmission Laboratory (A-METLAB) of RISH, Kyoto University by WiPoT, Kyoto Univ., Mini-Surveyor Consortium, and Autonomous Control Systems Laboratory Ltd. 5.8 GHz, 8.74W microwave power was transmitted from 8 × 8 array antenna (21 dBi) on a flying drone (multicopter) as shown in Fig. 1. Received and rectified 6.1 mW DC power drives a sensor. Hopeful applications of the Multicopter Assisted WBLS are rescue of victims, WPT-powered sensors at volcano, and inspection of infrastructures (bridges, tunnels), etc.

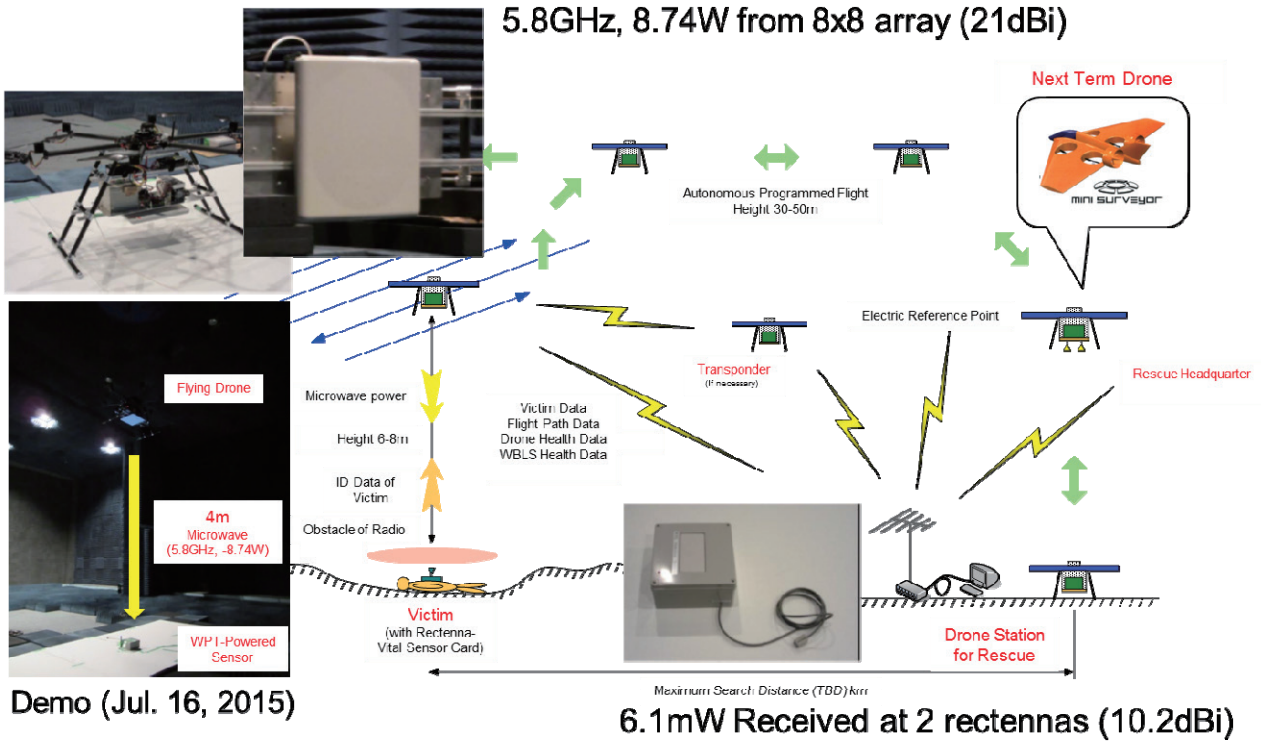

Fig.1. Concept of Multicopter Assisted WBLS and its demonstration on July, 2015 at A-METLAB

Acknowledgements

Part of this research was carried out by use of Microwave Energy Transmission Laboratory (METLAB) as collaborative inter-university research facility.

RECENT RESEARCH ACTIVITIES

Novel Space Environment Monitor, Instrument, and Space Mission Concepts

(Laboratory of Space Systems and Astronautics, RISH, Kyoto University)

Hiroshi Yamakawa, Hirotsugu Kojima, and Yoshikatsu Ueda

Space Debris Observation, Modelling, and Mitigation

The space debris problem is tackled from observation (space situational awareness), trajectory evolution, and mitigation points of view. 1) A method to identify the size, shape, and rotation, and to determine the trajectory of known space debris using MU (Middle and Upper) Radar of RISH, Kyoto Universiry, is investigated with some successful observation results. 2) An on-orbit space debris observing system is studied assuming an optical sensor onboard a satellite. The required specifications of optical sensors and ranges of observable space debris are investigated. 3) A study has started to investigate space debris trajectory evolution focusing on objects smaller than 10 cm. 4) Space debris mitigation (orbit control) using Lorentz force by positive charging effect is studied. Lorenz force is based on the interaction between an electro-statically charged debris and the Earth's plasma environment. The orbit control method to decrease the altitude using Lorentz force is studied focusing on decreasing semi-major axis, enlarging eccentricity, and lowering perigee distance.

Electric Sail and Magneto-Plasma Sail Space Propulsion System

An Electric Sail (ES) is a space propulsion system by positively charging the extended wires attached to the spacecraft body, which captures the momentum of the solar wind. The thrust of the ES is evaluated and applied for deflecting near-Earth asteroids which has a possibility of approaching the Earth in the near future. Another space propulsion system studied is a Magneto-Plasma Sail (MPS) is a unique propulsion system, which travels through interplanetary space by capturing the energy of the solar wind, which inflates a weak original magnetic field made by a High-Temperature Super-conducting (HTS) coil of several m in diameter with an assistance of a high-density plasma jet. We investigated the methods to maximize the thrust capability by increasing the thrust to mass ratio. The approaches we took are 1) optimizing the HTS coil design to increase the current and maximize its magnetic moment within the capacity of the space vehicle, and 2) developing a deployable HTS coil with a larger diameter to increase the coil area and magnetic moment in space.

Miniaturization of plasma wave receiver system

To meet the recent requirements on the size, mass and power budgets in constellation missions or planetary missions, the miniaturization of plasma wave receiver is inevitable. The attempt to realize the extremely miniaturized plasma wave receiver have been made using analogue ASIC technology in the lab. The main activity in 2012 is the success in the development of the tiny waveform capture receiver, which is one of the typical types of plasma wave receivers. The size of the developed tiny waveform receiver is about one tenth of the conventional waveform receiver. Moreover, we also succeeded in implementing the preamplifier and the calibration system on the same analogue chip of the waveform receiver.

Quantitative evaluation of electrochemical properties of fine-bubbles in water based on the type of gas

Recently, fine bubble (FB) has found applications in various fields. We have reported the effectiveness of water containing FB water of approximately 100 nm diameter for removal of radioactive cesium from soil and gravel conglomerate and nonwoven cotton. In Fukushima, this method of radioactive contamination removal using FB water is currently under trial. We also investigated the freshness-keeping effect of water containing FB on cut flowers such as a gentian, a lisianthus, and a small chrysanthemum. Although there were statistical dispersions in experimental results, FB was effective in keeping the freshness in the experiments. We focused our attention on the electrochemical properties of pure water (such as pH and electrical conductance) containing FB; we evaluated their correlation with the concentration of FB and investigated their potential for use as parameters for the characterization of FB in water.

ABSTRACTS (PH D THESIS)

Studies on coumarin-specific prenyltransfrase genes in plants

(Graduate School of Agriculture, Laboratory of Plant Gene Expression, RISH, Kyoto University)

Ryosuke Munakata

Introduction

Coumarins are a large natural product group consisting of more than 1,500 derivatives as being plant secondary phenolics, and they contribute to chemical defense mechanism against a variety of environmental stresses, such as pathogens, herbivores, and abiotic stresses (ref. 1). Prenylation reactions largely diversify the chemical structures and bioactivities of coumarins, while none of prenyltransferase (PT) genes for coumarins have been identified thus far. In this study, we have performed molecular isolation, characterization, and phylogenetic analysis of PT genes characteristic to coumarins in order to elucidating prenylation reaction that is playing important roles in coumarin biosynthesis.

Geranyl diphosphate-specific coumarin PT from lemon

So far, almost all of plant-derived PT genes for aromatics encode membrane-bound enzymes accepting dimethylallyl diphosphate (DMAPP, C_5) as their specific prenyl donor. It is to be noted that they have been isolated from Fabaceae in most cases. Therefore, cDNA cloning of PT accepting longer prenyl donor, *e.g.*, geranyl diphosphate (C_{10}), was carried out using new plant taxon as its gene source.

Lemons (*Citrus limon*, Rutaceae) accumulate large amounts of geranylated coumarins in their outer pericarp, flavedo. Homology-based PCR cloning was done using cDNA pool from lemon flavedo and degenerated primers designed on conserved amino acid regions among known PT members. As a result, a strong candidate gene, *C. limon PT1* (*ClPT1*) encoding a hydrophobic polypeptide with 407 amino acids, was isolated. ClPT1 has two aspartate-rich motifs well conserved in the aromatic PT family, and i*n silico* analysis predicted that ClPT1 has plastid-sorting signal at its N-terminal region and multiple transmembrane helices. Biochemical studies using a yeast recombinant protein indicated that ClPT1 shows geranyltransferase activities for coumarin derivatives. Further enzymatic properties of this membrane-bound enzyme were preformed.

O-PT for aromatics

In general, *Citrus* species accumulate various *O*-prenylated coumarins, such as bergamottin, where prenyl moieties were attached to benzene ring via *C*-*O* bond, while no genes corresponding to the C-O bond-mediated prenylation for aromatics has been identified in plants so far. To obtain biochemical information of *O*-PT, enzymatic properties of the *O*-PT activity to yield bergamottin, bergaptol-5-*O*-geranyltransferase (B5OGT) activity, was investigated using crude enzyme prepared from lemon flavedo. B5OGT activity was detected only from membrane fraction of lemon flavedo and required divalent cations, *e.g.* Mg^{2+} and Mn^{2+}. Both properties were common to already-known aromatic PT members in plants, suggesting that *O*-PT genes in Rutaceae belong to membrane-bound PT gene family.

PT genes involved in the first reaction step in furanocoumarin formation

Furanocoumarins (FC), a tricyclic coumarin subgroup composed of liner and angular types, function as defense chemicals against biotic stresses. In FC biosynthetic pathway, umbelliferone dimehylallyltransferase (UDT), a PT catalyzing the first reaction step, determines which FC types is finally produced, i.e., dimethylallyltransferase activity at 6 or 8-position of umbelliferone (U6DT or U8DT activity) yields demethylsuberosin or osthenol leading to linear or angular FC, respectively (Fig. 1). In this study, identification of UDT genes from parsnip (*Pastinaca sativa*, Apiaceae) was performed. *In silico*

screening of EST data constructed from parsnip total RNA found two candidate cDNAs, *P. sativa PT1* and *2 (PsPT1* and *PsPT2*). *In vitro* characterization of PsPT1 and PsPT2 using *Nicotiana benthamiana* transient expression system revealed that PsPT1 and PsPT2 show U6DT and U8DT activities as their major function. Expression of both *PsPT1* and *PsPT2* was induced by methyl jasmonate, a FC elicitor, suggesting their involvement in FC biosynthesis. Moreover, when crude enzyme from parsnip was incubated with DMAPP and umbelliferone, much higher U6DT activity than U8DT activity was detected, suggesting a possibility that PsPT1 is the major UDT in parsnip.

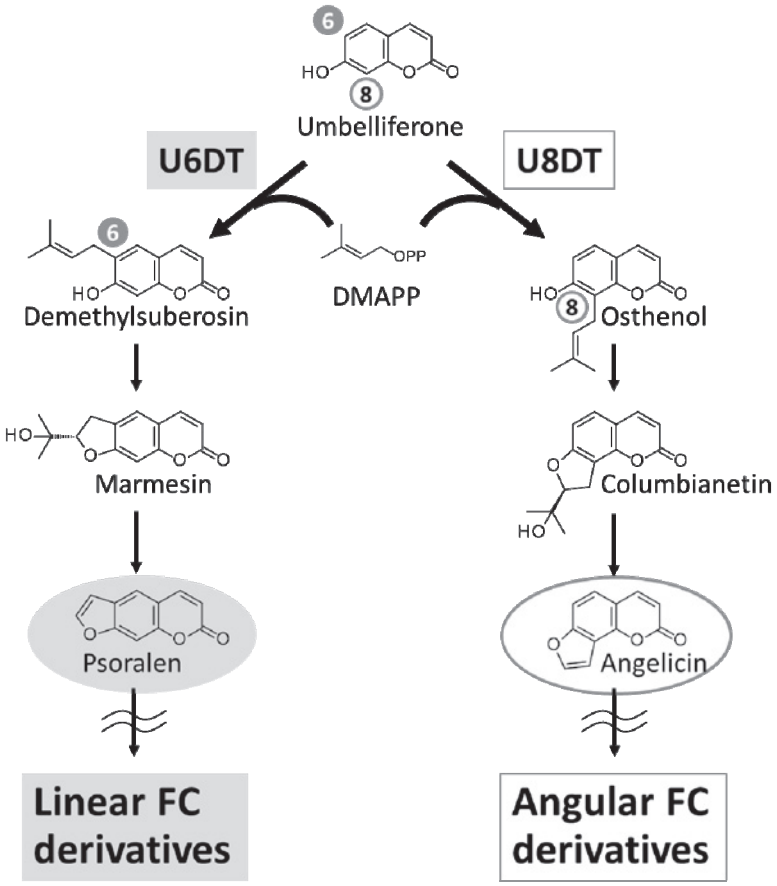

Fig. 1 Furanocoumarin biosynthetic pathway
Psoralen and angelicin were core structures of linear and angular FCs, respectively.

Reference

[1] Bourgaud, F., Hehn, A., Larbat, R., Doerper, S., Gontier, E., Kellner, S. and Matern, U., Biosynthesis of coumarins in plants: a major pathway still to be unravelled for cytochrome P450 enzymes, *Phytochemistry Reviews*, 5: 293 – 308, 2006.

ABSTRACTS (PH D THESIS)

A study of water vapor variability associated with deep convection using a dense GNSS receiver network and a non-hydrostatic numerical model

**(Graduate School of Science,
Laboratory of Atmospheric Sensing and Diagnosis, RISH, Kyoto University)**

Masanori Oigawa

The characteristics of water vapor variability associated with the initiation and evolution of deep convection were investigated by using Global Navigation Satellite System (GNSS) meteorology technique and a meso-scale non-hydrostatic numderical model (NHM). The local scale spatio-temporal variability of precipitable water vapor (PWV) was analyzed by using a dense GNSS receiver network installed around Uji, Kyoto, with inter-station distances of about 1-2 km. The PWV data were used to validate the NHM results and to investigate the optimum scales of water vapor measurement for predicting deep convection by conducting a data assimilation experiment. Next, an observational campaign was conducted in Indonesia to elucidate the feasibility of GNSS meteorology and meso-scale NHM in the tropical region.

First, observational system simulation experiments (OSSE) were performed to investigate the improvement of local-scale PWV measurement due to increased horizontal resolution of GNSS-derived PWV. Local-scale PWV fluctuations were smoothed out previously, because all slant path delays above a low elevation (5°−10°) cut off were averaged to estimate a single PWV value in the conventional procedure. In this study, only high elevation Quasi-Zenith Satellite System (QZSS) (higher than 80°) and GPS (higher than 60°) were selectively used to estimate PWV. The simulation result showed that meso-γ scale PWV fluctuations can be observed by this method.

Secondly, a case study was conducted to understand the mechanisms of PWV variation during a heavy rainfall event on 14 August 2012 in Uji, by comparing the GNSS-PWV and the downscaled 250 m mesh model data. Although a simulated convection was initiated at slightly different place and time from the observation result, the model successfully simulated the observed rapid increase of PWV prior to the surface rainfall. In the model, the local PWV maximum began to form about 16 min before the surface rainfall due to wind convergence near the ground. Five minutes later, free convection was initiated at approximately 1 km elevation by the preceding surface wind convergence. Due to the existence of a stable inversion layer between 2.2 and 3.5 km elevation, the shallow free convection took 11 min to rise above the inversion layer to form a deep convection. It was found that low-level wind convergence caused the local increase of PWV prior to generation of deep convection.

Third, the high-resolution PWV data derived from the Uji network were assimilated to a nested NHM-LETKF system, and the optimum scales of water vapor measurement for predicting deep convection was investigated. From the analysis of the observed Zenith Wet Delay derived from the Uji network, it was found that horizontal scale of water vapor variability became small (1.9-3.5 km) when it rained around the Uji network. The data assimilation experiments showed that simulation accuracy of one hour accumulated rainfall amount was most improved when the PWV data were assimilated with horizontal resolution of 3.5 km that was consistent with the observed horizontal scale of the water vapor valiability. In addition, it was found that influence of observation error correlation of PWV can become smaller by

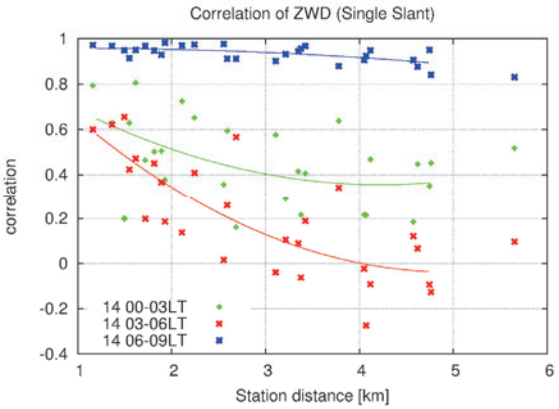

Figure 1. Horizontal distance dependency of correlation of ZWD converted from highest elevation single slant delays derived from the Uji network during rain-free (blue), weak rain (green), and heavy rain (red) periods. Curves are fitted second degree polynomials.

assimilating PWV which were converted from highest elevation single slant delays instead of using conventional PWV data. Analysis of the assimilated model data revealed that the observed local PWV increase at the north edge of the rain band was formed by wind convergence above planetary boundary layer induced by clockwise rotating vertical wind shear.

Based on these outcomes, the studies using GNSS meteorology method and NHM were applied to Indonesia which is the most active convective region in the world, because GNSS receiver networks are rapidly being constructed whereas operational meteorological networks are insufficient. An intensive observation campaign using GNSS receivers, radiosondes, and X-band Doppler radar was carried out in 2013 in the Bandung basin which is as small as about 20 km. Relations between water vapor variability inside the small basin and convective initiation was investigated by analyzing the observation data and downscaled NHM data. The model results successfully reproduced the observed deep convection and showed that static stability around the southern slope of the basin decreased due to moisture transport from the bottom basin by a thermally-induced circulation that formed low-level wind convergence with deepened moist convective mixed layer at the southern basin and decreased moisture at the northern basin. The simulated local-scale water vapor variability was also observed by the GNSS receiver network. It was suggested that water vapor at the bottom basin in the morning and low-level wind convergence induced by the local circulation are important for convection initiation in Bandung.

This is the first study that demonstrated that high-resolution PWV data assimilation with inter-station distances of less than 10 km can improve simulation accuracy of localized heavy rainfall. The revealed characteristic scale of water vapor variability and optimum scale for PWV assimilation was about 3.5 km. The use of a dense GNSS receiver network and high elevation GNSS satellites like QZSS is the best way to retrieve the local scale water vapor variability and it is important to assimilate the high resolution PWV data into a numerical weather prediction model.

ABSTRACTS (PH D THESIS)

Investigation of natural adhesive composed of tannin and sucrose for particleboard

(Graduate School of Agriculture, Laboratory of Sustainable material, RISH, Kyoto University)

Zhongyuan Zhao

Wood-based materials are generally used in housing construction and furniture manufacture, and they are frequently present in living environments. In the wood industry, wood adhesives are necessary to obtain satisfactory physical properties of the wood-based materials. Usually, the synthetic resins are used during the manufacture of the wood-based materials, such as formaldehyde-based, polyvinyl acetate (PVAc), isocyanate based resin and so on. These synthetic resins are mostly based on the chemical substances which derived from fossil resources; however, it is believed that the use of the current wood adhesives will be unavoidably restricted in the future due to decreases in the reserves of fossil resources. In this study, tannin and sucrose were chosen as the adhesive component. In the first place, the weight ratio of adhesive compounds, mat moisture content, the effects of hot pressing temperature, hot pressing time and resin content on the physical properties of the particleboard bonded by tannin and sucrose were investigated, based on the results, the optimal manufacture conditions were obtained. Secondly, the thermal analysis, insoluble matter and FT-IR analysis were carried out to study the curing behavior of tannin and sucrose. Finally, based on the results of reaction mechanism of tannin and sucrose, citric acid was added to reduce the reaction temperature of tannin and sucrose.

Results and discussion

(1) Effects of pre-drying treatment, mixture ratio and resin content on physical properties of the particleboard bonded by tannin and sucrose [1]

Tannin and sucrose were used as adhesives to manufacture the particleboard, and we investigated the tannin/sucrose ratio, effects of the drying treatment after spraying and resin content on particleboard properties. As the results, the properties were enhanced when the drying treatment was carried out after the spraying, and when the sucrose ratio increased. Based on the results obtained, the optimum proportion of tannin to sucrose was 25/75, and the optimum resin content was between 30 wt% and 40 wt%. When the particleboards were manufactured under the optimum conditions, the maximum MOR, MOE, and IB are 21.3MPa, 5.0 GPa, and 1.3MPa, respectively. The results showed excellent mechanical properties, higher than those required for JIS A5908 type 18. Based on the results of FT-IR, 5-HMF was formed from the decomposition of sucrose during the heating treatment. In addition, as one kind of the possible reaction mechanism between tannin and sucrose, the dimethylene ether bridges seems to be formed. The possible reaction mechanism was shown in Figure 1.

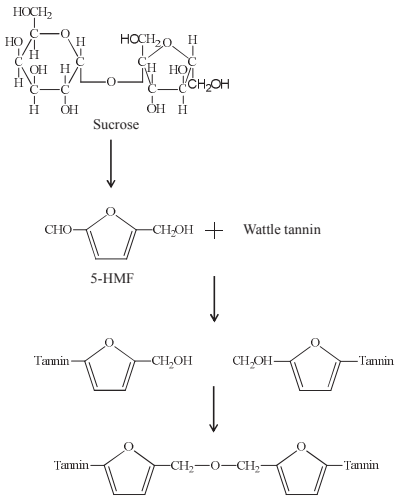

Figure 1. Possible reaction equation between tannin and sucrose.

(2) Effects of pressing temperature and time on particleboard properties, and characterization of tannin-sucrose adhesive [2]

The effects of hot pressing temperature and hot pressing time on the physical properties of the boards were investigated. The mechanical properties and water resistance increased as the hot pressing temperature and time increased. The optimum hot pressing temperature was 220°C, and the optimum hot pressing time was 10min. The MOR, MOE, IB and TS of the board manufactured under the optimum

condition were 23.5MPa, 5.3GPa, 1.6MPa, and 7%, respectively, which were higher than the requirement of the 18 type of JIS A 5908. Thermal analysis showed that the endothermic reaction of the adhesive composed with tannin and sucrose (only the ratio at 25/75) were happened at more than 200°C, this explaining the promotion of the particleboard properties when the hot pressing temperature was increased to 220°C. When the heating time was longer than 10min, insoluble matter was higher than 70wt%. The FT-IR results (Figure 2) showed the existence of the furan ring (1509 and 780 cm^{-1}), carbonyl group (1705 cm^{-1}) and dimethylene ether bridges (1200 cm^{-1}) in the cured adhesives. Comparing the FT-IR spectra of the adhesives heated in different heating time, there was not obviously change of chemical structure in the hot pressing time range of 10-20min.

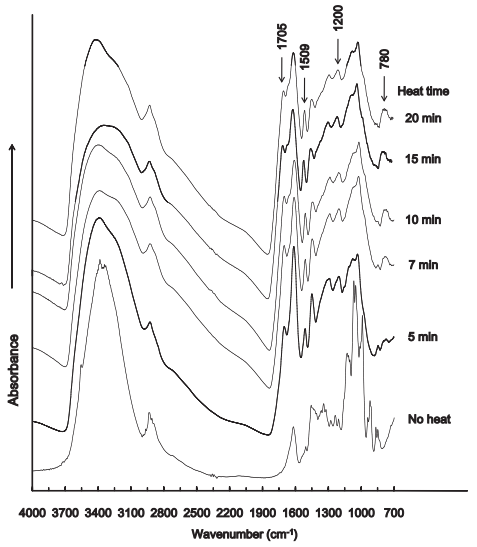

Figure 2. FT-IR curves of the adhesives cured at 220℃.

(3) Effects of addition of citric acid on physical properties of particleboard using tannin sucrose adhesive [3]

To reduce the hot pressing temperature of the particleboard bonded by tannin and sucrose, citric acid was incorporated into a tannin and sucrose adhesive, and the effect of this addition on the hot pressing temperature of particleboard was investigated. The results showed that the addition of citric acid was effective in reducing reaction temperature, and the insoluble matter remaining from 20.0 and 33.3 % citric acid contents adhesives at 200 °C was 2 times higher than for the tannin-sucrose adhesive. In addition, the results of the FT-IR analysis on the adhesives added citric acid and heated at 200°C (Figure 3) showed that the peaks of ester linkage (1731 cm^{-1}) and dimethylene ether bridges (1200 cm^{-1}) increased as the increasing of citric acid content. The physical properties of the particleboards bonded with tannin-sucrose-citric acid adhesive with 20.0 and 33.3 % citric acid contents at more than 200 °C satisfied the requirements of the type 18 standard of JIS A 5908 (2003). Consequently, the addition of citric acid promoted the reaction between tannin and sucrose at a lower temperature, and decreased the hot pressing temperature to 200 °C, while enhancing the bending properties at 220°C.

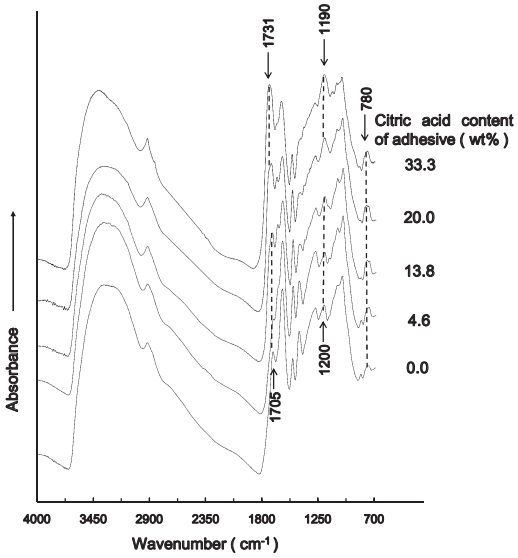

Figure 3. FT-IR curves of the tannin-sucrose adhesives added citric acid and heated at 200℃.

References

[1] Zhao, Z., Umemura, K. Investigation of a new natural particleboard adhesive composed of tannin and sucrose. Journal of Wood Science. 60, 269-277. June 2014.

[2] Zhao, Z., Umemura, K. Investigation of a new natural particleboard adhesive composed of tannin and sucrose 2: Effect of pressing temperature and time on board properties, and characterization of adhesive. BioResources, 10(2), 2444-2460. February 2015.

[3] Zhao, Z., Umemura, K., Kanayama, K. Effects of the addition of citric acid on tannin-sucrose adhesive and physical properties of the particleboard. BioResources, 11(1), 1319-1333. December 2015.

ABSTRACTS (PH D THESIS)

Production of aromatic compounds and functional carbon materials by pulse current pyrolysis of woody biomass

(Graduate School of Agriculture, Laboratory of Innovative Humano-Habitability, RISH, Kyoto University)

Sensho Honma

The development of technologies for obtaining useful chemical substances from sources other than fossil resources has received worldwide attention. In particular, there is a need for the production of feedstock chemicals from abundant wood biomass. Pyrolysis is an important technology involving the quick and efficient conversion of biomass materials to chemicals. Pyrolysis of wood biomass generates viscous pyrolysis oil and char with unique properties like surface properties and pore characteristics within extremely short time periods. Collection and utilization of both char and pyrolysis oil are also necessary for the efficient production of useful chemical substances. Hence, precise control over pyrolysis conditions and the use of an optimal catalyst are necessary to selectively promote the pyrolysis reaction. Pyrolysis employing the pulse current heating method can be applied to satisfy these requirements in the selective conversion of wood biomass to useful chemical substances. The optimization of pyrolysis conditions is necessary for improving the applicability of this heating method in the production of pyrolysis oil and char with the required characteristics.

This research was carried out for the purpose of utilizing both pyrolysis oil and char that were obtained from woody biomass, and for selectively producing functional carbon composite materials and pyrolysis oil containing useful compounds. The pyrolysis products were characterized, and the effects of the pyrolysis conditions on product distribution, pyrolysis oil composition, and carbon composite material composition were investigated.

In Chapter 1, we have applied rapid pyrolysis by pulse current heating for this purpose. Japanese cedar wood was pyrolyzed at various temperatures, and the compositional and structural changes in the degraded products were characterized using GC-MS, FT-IR, Raman spectroscopy, and elemental analysis. We found that ammonia was adsorbed on the char obtained by the pyrolysis at 500 °C and observed a sharp dependence of the adsorptivity on the pyrolysis temperature (Fig. 1). Under this condition, phenolic compounds such as guaiacol, catechol, 4-vinyl guaiacol, and vanillin were produced as the major components of the pyrolysis oil (Fig. 2). Deoxygeneation proceeded linearly as a function of the pyrolysis temperature and that pyrolysis at 800 °C produced aromatic hydrocarbons such as naphthalene, acenaphthylene, anthracene, and pyrene along with the current platform chemicals such as benzene, toluene, and styrene (Fig. 2). The functionality of residual char as an ammonia adsorbent and the co-production of aromatic chemicals can be highlighted as a new process designed for efficient usage of woody biomass.

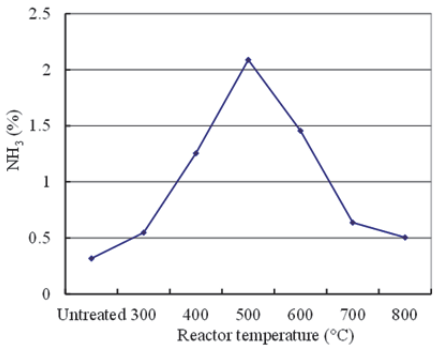

Fig. 1. Adsorption of ammonia on the char obtained from Japanese cedar wood meal pyrolyzed in the range of 300–800 °C.

In Chapter 2, the relationship between adsorption ability and pyrolysis conditions for Todo-fir char was investigated. Pyrolysis under an air atmosphere was effective in generating acidic functional groups such as carboxylic acid groups, and it improved the properties of the Todo-fir char. A pyrolysis temperature of 300 °C was found to be most effective, and the change in the chemical structure of cellulose was reflected in the formation of acidic functional groups by the pyrolysis of Todo-fir in air. From these results, it was concluded that pyrolysis under an air atmosphere was effective in generating acidic functional groups such as the carboxyl group, which improved the ability of the product to adsorb basic substances

like ammonia.

In Chapter 3, the influence of catalysts on the compositions of char and pyrolysis oil obtained by pyrolysis of wood biomass with pulse current heating was studied. The effects of catalysts on product compositions were analyzed using GC-MS and TEM. The compositions of some aromatic compounds changed noticeably when using a metal oxide species as the catalyst. The coexistence or dissolution of amorphous carbon and iron oxide was observed in char pyrolyzed at 800 °C with Fe_3O_4. Pyrolysis oil compositions changed remarkably when formed in the presence of a catalyst compared to that obtained from the uncatalyzed pyrolysis of wood meal. We observed a tendency toward an increase in the ratio of polyaromatic hydrocarbons in the pyrolysis oil composition after catalytic pyrolysis at 800 °C. When iron oxides and TiO_2 were used as catalysts, the composition ratio of aromatic hydrocarbon compounds such as naphthalene was shown to increase, even at a processing temperature of 500 °C. Pyrolysis of biomass using pulse current heating and an adequate amount of catalyst is expected to yield a higher content of specific polyaromatic compounds.

In Chapter 4, the pyrolysis of rice husks, Todo-fir, and cellulose by pulse current heating was examined to elucidate the influences of reaction temperature on their product distributions and chemical properties of the resulting oil and char fractions for utilization of pyrolysis products obtained from biomass. Some common characteristics were found for each product distribution: The maximum yield of pyrolysis oil obtained from each material was observed at 500–600 °C. In contrast, the following characteristic properties of pyrolysis products obtained from each material were observed: High ash content and char yields at each processing temperature were found in the rice husk pyrolysis products. Aromatic hydrocarbons were detected in the pyrolysis oil obtained from rice husks at lower temperature pyrolysis. The yield of pyrolysis oil obtained from rice husks was lower than that from Todo-fir, and the yield of pyrolysis oil obtained from Todo-fir tended to be higher than those from rice husks and cellulose at all temperatures. Plenty of levoglucosan was detected in the pyrolysis oil obtained from cellulose at 500–800 °C, although the yield of the pyrolysis oil was not so high. In the pyrolysis oil obtained from rice husks, such aromatic hydrocarbons as benzene and styrene, as well as polycyclic aromatic hydrocarbons like naphthalene, phenanthrene, anthracene, and pyrene, were detected at 600–800 °C.

The chemical structure and microscopic structure of the carbon composite materials obtained at each pyrolysis temperature were shown by investigating the relationship between the pyrolysis conditions in the pulse current heating method and the catalytic effect of the metal oxide. Since suitable pyrolysis conditions for producing ammonia adsorbent and the characteristics of the metal oxide carbon composite material were shown, char obtained as a pyrolysis residue was considered to contribute to the production of a useful material in addition to pyrolysis oil. Moreover, this method was applied for the production of silica carbon composite material along with the pyrolysis oil, by using rice husk, a previously unutilized biomass, as the raw material. Accordingly, the results of this research are expected to contribute to the effective use of unused resources for producing pyrolysis oil containing useful compounds and functional carbon composite materials.

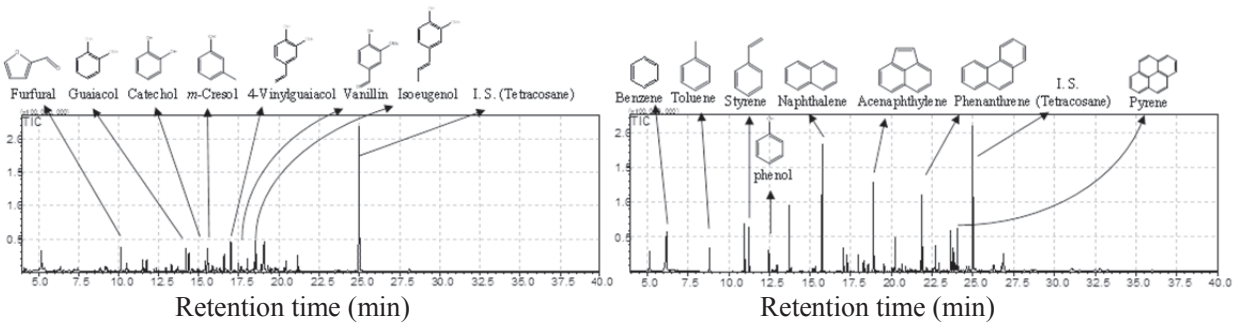

Pyrolyzed at 500 °C Pyrolyzed at 800 °C

Fig. 2. Total ion chromatogram (TIC) of pyrolysis oil obtained from Japanese cedar wood meal pyrolyzed at 500 °C and 800 °C by GC-MS.

ABSTRACTS (PH D THESIS)

Studies on mass culture and aggregation pheromones in the exotic powderpost beetle, *Lyctus africanus* Lesne (Coleoptera: Lyctinae)

(Graduate School of Agriculture, Faculty of Forest and Biomaterials Science, Laboratory of Innovative Humano-habitability, RISH, Kyoto University)

Titik Kartika

Lyctus africanus, a powderpost beetle belonging to Lyctinae subfamily in Bostrichidae family, is an important pest owing to its migration into new countries, and it has been considered to be one of the major pests threatening timber and wood products, including plywood, dried roots, seeds and tubers. Lyctine damage is mostly identified belatedly by reason of poor knowledge and skill to locate and monitor the infestation. Unfortunately, there is still no device for detecting and monitoring Lyctine beetles in the field due to the lack of sufficient data on their ecological features. Thus, strategies for monitoring and controlling this beetle by examining the Lyctine ecology are urgently needed. To accomplish the study, establishment of the mass culture of *L. africanus* was also elaborated. This study aims at the establishment of the mass culture and monitoring system for *L. africanus*.

To establish the mass culture of *L. africanus*, the significance of artificial diet quality toward fecundity and also population of the *Lyctus* were evaluated to find standard diet for rearing *L. africanus* in laboratory before conducting further study on aggregation behavior of *L. africanus*.

In experiment, the usefulness of some artificial diets with different fillers were evaluated to improve the growth of *L. africanus*. *L. africanus* were raised in three types of diets (wood- [Diet 1], and celluolose- [Diet 2 and Diet 3] based diet). A group of five females and males *L. africanus* were liberated onto the diet and allowed to complete the life cycle. The new generations were harvested and then subjected to several experiment, such as oviposition test, total population measurement and also determination of sex ratio and body weight of the beetle.

The number of laid eggs and survived adults after oviposition test were observed. The results revealed that combination of starch and sugar acted as oviposition stimulant for *Lyctus* adults emerged from Diet 1, Diet 2, and Diet 3. The adults emerging from cellulose-based diets (Diet 2 and Diet 3) were likely to oviposit more eggs than what Diet 1-emerged adult did, which indicated that cellulose might support the oviposition ability of *L. africanus*. However, all adults emerging from three diets survived in the same values after laying eggs on both oviposition sites.

Furthermore, the newly emerged beetles were harvested and observed the total population of larvae, adults, as well as sex ratio and body weight measurement. The results on larval number indicated that total larvae was similar among the three diets. For adult stage, sex ratio and body weight of *L. africanus* were similar among the three diets, however, the total adults was significantly lower in the Diet 3 than the other diets (Table 1). It was suggested that the amount of vital nutrient (starch) in the diet is not the only important factor to be considered when selecting a diet for *L. africanus*. The filler should also enhance oviposition potential and larval development. Hence, Diet 1 and Diet 2 could be used alternately for rearing *L. africanus* in laboratory.

Then, the aggregation behavior of *L. africanus* to develop a monitoring technique for the beetle was investigated by chemical approach through comprehensive screening of the potential compound produced by *L. africanus*. The whole body extractions using hexane solvent on newly emerged beetles were performed. The aggregation activity of crude extract of *L. africanus* beetles was conducted by dual-choice bioassay. Then, it was followed by chemical analysis, isolation, identification and syntheses of the chemical compounds. The results revealed three esters as an aggregation pheromone produced by male *L. africanus* beetle. The esters were recognized as a major compound **2** (3-pentyl dodecanoate) and two minor compounds **1** and **3** (2-propyl dodecanoate and 3-pentyl tetradecanoate) based on its quantitative amount in the crude extract (Figure 1).

ABSTRACTS (PH D THESIS)

Table 1. Development of *L. africanus* in three artificial diets

Artificial diet	Total adults	Sex ratio (M/F)	Body weight (mg)
Diet 1	206.0 ± 49.37[a]	0.94 ± 0.06[a]	1.98 ± 0.04[a]
Diet 2	188.9 ± 30.60[a]	0.80 ± 0.05[a]	1.87 ± 0.06[a]
Diet 3	55.9 ± 16.18[b]	0.76 ± 0.08[a]	2.01 ± 0.21[a]

Note: a.b significantly different in the same column by Tukey-Kramer HSD test ($P < 0.05$).

To justify the significant role of the synthetic esters to *L. africanus* the aggregation activity of either single or blended esters was evaluated. The bioassays were conducted in laboratory by dual-choice test against *L. africanus* beetles. The results indicated that the single compound was not sufficient to induce the aggregation behavior of *L. africanus*. Furthermore, the natural blended compound increased the aggregation responses of *L. africanus*. There was a synergistic effect was found among the three synthetic esters.

A semi-field test was carried out in order to initiate a pheromone-based monitoring program in the future. The optimum dose of three-ester blend was determined using dual-choice test. The blend of three synthetic esters were prepared to determine the minimum dosage that elicited the maximum level of response from both female and male *L. africanus* beetles. Consequently, the optimum dose inducing greatest aggregation response on *L. africanus* was applied for wind-tunnel bioassay.

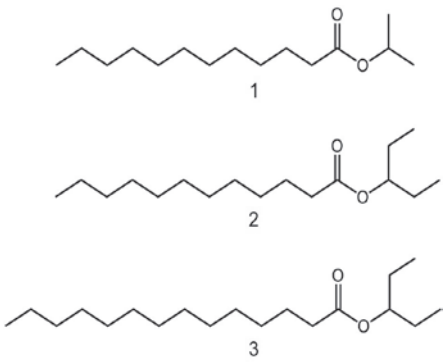

Figure 1. Chemical structures of compounds
(1) 2-propyl dodecanoate;
(**2)** 3-pentyl dodecanoate ; and
(**3)** 3-pentyl tetradecanoate

Results of dual-choice bioassays indicated that 50 BE induced the greatest response of aggregation behaviour of *L. africanus*. Furthermore, the wind tunnel bioassays revealed that both female and male beetles showed arousal response toward the natural blend of esters, however the male were less responsive than the female *L. africanus* beetles. The aggregation pheromone might efficiently perform on female rather than male *L. africanus* beetles.

These results indicated the potential ability of ester compounds as aggregation pheromones of *L. africanus* to be developed as an attractant in insect monitoring. Additional studies are still necessary to strengthen the performance of synthetic esters for establishing the monitoring system of *L. africanus*.

ABSTRACTS (PH D THESIS)

Study on Beam Forming for Phased Array Antenna of Panel-structured Solar Power Satellite

(Graduate School of Engineering, Laboratory of Applied Radio Engineering for Humanosphere, RISH, Kyoto University)

Takaki Ishikawa

A solar power satellite (SPS) is a huge satellite designed as an electric power plant in a geostationary Earth orbit. The SPS generates electricity using solar cells in outer space and transmits the generated electricity to a receiving site on the Earth through microwave power transmission. A panel-structured SPS corresponds to the main structure of a tethered SPS. The transmission antenna of the panel-structured SPS is a phased array antenna, consisting of many antenna elements. The radiation pattern of the phased array antenna can be manipulated by controlling the output phases and the power of microwaves radiated from each antenna element. The panel modules are connected exibly, and the shape of the panel-structured SPS is easily deformed (Fig.1). When the shape of the panel-structured SPS is deformed, the beam shape of the power transmission microwave is deformed due to errors caused by the change in the positions of the antenna elements. Hence, this deformation must be corrected for electricity to be transmitted with high efficiency.

First, in this study, we perform experiments using an actual phased array antenna consisting of 256 antenna elements and we simulate the beam forming using the experimental phased array antenna. The results of these experiments incdicate that we can control the radiation patterns and the beam direction with exceedingly high accuracy using current technology. Moreover, by comparing the experimental with the simulation results, we confirm that we can simulate the radiation patterns with high accuracy. We then simulate the radiation pattern of the phased array antenna on the panel module of the panel-structured SPS. The results indicate that the peak directivity is decreased to 90% when the size of the beam direction is 30◦ and is decreased to 50 % when the size of the beam direction is 40^{o}.

Second, we evaluate the position and angle correction (PAC) method, which was proposed for the phased array antenna of the panel-structured SPS. The PAC method estimates the positions of the antenna elements and calculates the correction values of the output phases from the pilot signal that is radiated from the receiving site on the Earth in order to detect the receiving site. A simplified simulation model, which corresponds to a panel structured SPS consisting of panel modules with a linear phased array antenna, is constructed to simulate the PAC method. The simulation results confirm that the PAC method can be applied to correct the beam shape, even if the pilot signal phase measurement contains errors. Moreover, when the distance between the pilot signal receiving points widens, the size of the phase correction errors decreases. In fact, when the standard deviation of the phase measurement errors is defined as 10^{o} and the pilot signal receiving points are placed at the ends of each panel module, the standard deviation of the output phase correction errors is approximately 16^{o}.

Third, we propose and evaluate ambiguity elimination methods for the angle estimations of the panel modules in the simplified simulation model. From the previous evaluations, the distance between the pilot signal receiving points must be widened to improve the phase correction accuracy of the PAC method. However, when the distance between the pilot signal receiving points is longer than half the wavelength of the pilot signal, the angle estimation of the panel module may fail due to ambiguities in the phase measurement of the pilot signal. Hence, we increase the number of pilot signal receiving points, and the ambiguities are eliminated by an unequal interval array of pilot signal receiving points. Evaluating the ambiguity elimination methods with three and four pilot signal receiving points, we confirm that the ambiguities can be perfectly eliminated using four pilot signal receiving points (Fig.2). We then propose an ambiguity elimination method with a flatness maintaining system. Evaluating the ambiguity elimination method with the atness maintaining system, we confirm that the ambiguities can be perfectly eliminated using the flatness maintaining system and three pilot signal receiving points.

Finally, we consider the pilot signal receiving antennas. A patch antenna is used as a power transmission antenna in the panel-structured SPS. Here, we propose using a patch antenna as a pilot signal receiving antenna. We design antennas to equalize the size of pilot signal receiving antennas and power transmission antennas. Thus, the power transmission antenna is replaced with the pilot signal receiving antenna, and the output phases are corrected by the PAC antenna in the panel-structured SPS. We simulate the mutual coupling effect in the pilot signal phase measurement. From the simulation, the mutual coupling is found to have little effect on the pilot signal phase measurement when the pilot signal phase receiving antenna is not adjacent to other pilot signal receiving antennas.

Furthermore, the ambiguity elimination methods can be used when we use the pilot signal receiving antennas in the PAC method, and we confirm that the patch antenna can be used as the pilot signal receiving antenna in the panel-structured SPS.

Acknowledgements

Part of this research was carried out by use of Microwave Energy Transmission Laboratory (METLAB) as collaborative inter-university research facility.

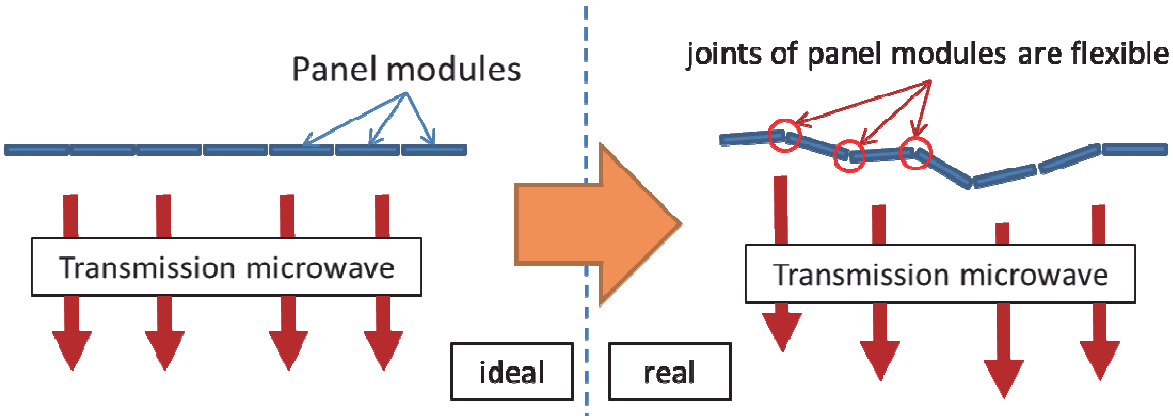

Fig.1. Concept of Panel Structure Antenna for SPS

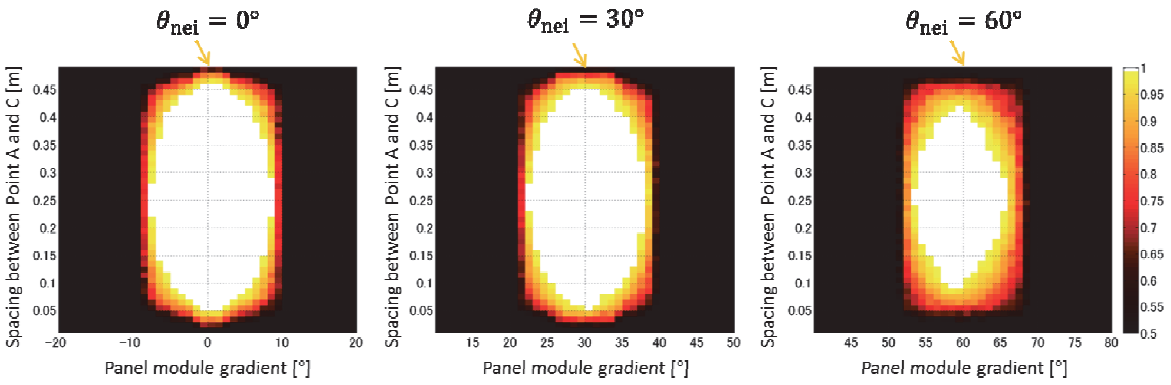

Fig.2. Result of ambiguity elimination method

ABSTRACTS (PH D THESIS)

Study on RF Safety by Using Human Cells in Vitro under Magnetic Resonant Coupling Wireless Power Transfer

(Graduate School of Engineering, Laboratory of Applied Radio Engineering for Humanosphere, RISH, Kyoto University)

Kohei Mizuno

Wireless power transfer (WPT) technology using the resonant coupling phenomenon has been widely studied. However, possible relationships between WPT exposure and human health have not been experimentally evaluated. In this study, we developed a new in vitro exposure system to evaluate the biological effects of magnetic resonant coupling WPT (Fig.1). The WPT was carried out using a self-resonant helical coil, which was designed to transfer the power with 85.4% efficiency at a 12.5 MHz resonant frequency. The magnetic field at the positions of the cell culture dishes is approximately twice the reference level for occupational exposure as stated in the International Commission on Non-ionizing Radiation Protection (ICNIRP) guidelines. The specific absorption rate (SAR) at the positions of the cell culture dishes match the respective reference levels stated in the ICNIRP guidelines. In this paper, the coil design for magnetic resonant coupling in the in vitro exposure system and characteristics, such as power transfer efficiency, electric field and magnetic field distributions and SAR of the exposure system, are described.

Next, we investigated whether exposure to magnetic resonant coupling WPT has genotoxic effects on WI38VA13 subcloned 2RA human fibroblast cells. WPT exposure was performed using a helical coil-based exposure system designed to transfer power with 85.4% efficiency at a 12.5-MHz resonant frequency. The magnetic field at the positions of the cell culture dishes is approximately twice the reference level for occupational exposure as stated in the International Commission on Non-ionizing Radiation Protection (ICNIRP) guidelines. The specific absorption rate at the positions of the cell culture dishes matches the respective reference levels stated in the ICNIRP guidelines. For assessment of genotoxicity, we studied cell growth, cell cycle distribution, DNA strand breaks using the comet assay, micronucleus formation, and hypoxanthine–guanine phosphoribosyltransferase (HPRT) gene mutation, and did not detect any significant effects between the WPT-exposed cells and sham-exposed cells. Our results suggest that WPT exposure under the conditions of the ICNIRP guidelines does not cause detectable cellular genotoxicity.

A dosimetric evaluation has also been discussed to evaluate the potential health risks of the electromagnetic field from this WPT technology based on the ICNIRP guidelines. However, there has not been much experimental evaluation of the potential health risks of this WPT technology. In this study, to evaluate whether magnetic resonant coupling WPT induces cellular stress, we focused on heat shock proteins (Hsps) and determined the expression level of Hsps 27, 70 and 90 in WI38VA13 subcloned 2RA human fibroblast cells using a western blotting method. The expression level of Hsps under conditions of magnetic resonant coupling WPT for 24 h (Tab.1) was not significantly different compared with control cells, although the expression level of Hsps for cells exposed to heat stress conditions was significantly increased. These results suggested that exposure to magnetic resonant coupling WPT did not cause detectable cell stress (Fig.2).

Acknowledgements

Part of this work was supported in part by a Grant-in-Aid for Scientific Research (B) (No.23310022) from the Japan Society for the Promotion of Science (JSPS) and a Development of New Research Area in Sustainable Humanosphere.

ABSTRACTS (PH D THESIS)

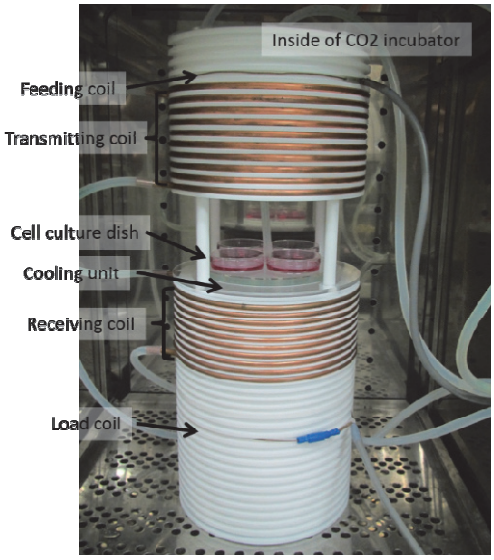

Fig. 1. Photograph of coils for magnetic resonant coupling WPT within the CO_2 incubator.

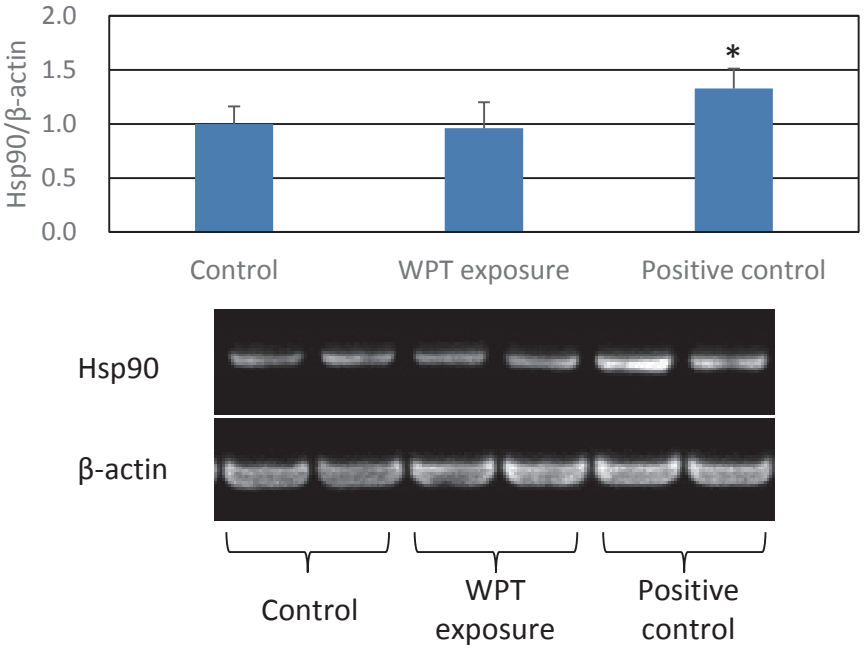

Fig 2. The expression of Hsp 90 in WI38VA13 subcloned 2RA human fibroblast cells exposed to WPT and control cells for 24 h, or heated at 43 °C as positive control. The expression of Hsp 90 was standardized to that of β-actin. Data are presented as means ± SD from three separate experiments. Photograph shows the typical results of Western blotting. * $p < 0.05$ compared with control.

ABSTRACTS (PH D THESIS)

Study on High Temperature Superconducting Coil System for Magneto Plasma Sail Spacecraft

(Graduate School of Engineering, Laboratory of Space Systems and Astronautics, RISH, Kyoto University)

Yoh Nagasaki

Superconducting coils can revolutionize space propulsion systems. The performances, e.g., acceleration and thrust to power ratio, of space propulsion systems can be greatly improved with a superconducting coil by generating a larger magnetic field with less power consumption and weight. A magneto plasma sail is a space propulsion system with a higher fuel efficiency or specific impulse for future deep space explorations. The thrust of the magneto plasma sail is produced by the transfer of momentum from a solar wind plasma to a strong magnetic field generated by a High Temperature Superconducting (HTS) coil as shown in Fig. 1. The thrust of the sail is proportional to the magnetic moment of the coil (coil turn number × coil current × area enclosed by the coil). To obtain a large thrust to mass ratio, or acceleration, enough for space missions, our target is to increase the magnetic moment to mass ratio of the HTS coil system ten times larger than that obtained by a previous study. The HTS coil system is optimized to maximize its magnetic moment to mass ratio within the capacity of a launch vehicle.

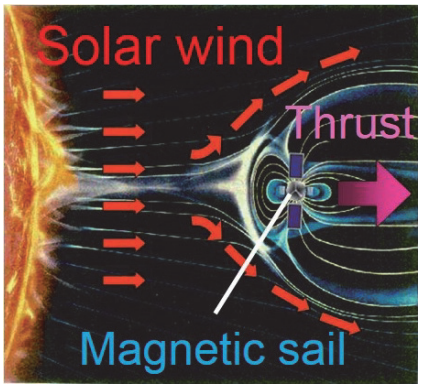

Figure 1. Thrust generation mechanism of the magneto plasma sail.

To design an HTS coil for the magneto plasma sail, we first investigated a quantitative current transport performance and thermal behavior of an HTS coil, and the effect of the critical current inhomogeneity along the longitudinal direction of HTS tapes on the coil performances. We measured the current transport property and temperature rises during current applications of a scale-down model HTS coil using a Bi-2223/Ag tape in a conduction-cooled system, and analytically reproduced the results on the basis of the percolation depinning model and three-dimensional heat balance equation. As a result, we precisely estimated the critical currents of the HTS coil within 10% error for a wide range of the operational temperatures from 45 to 80 K, and temperature rises on the coil during current applications as shown in Fig. 2. These results showed that our analysis and conduction-cooled system were successfully realized. The analysis also suggested that the critical current inhomogeneity along the length of the HTS tape deteriorated the current transport performance and thermal stability of the HTS coil.

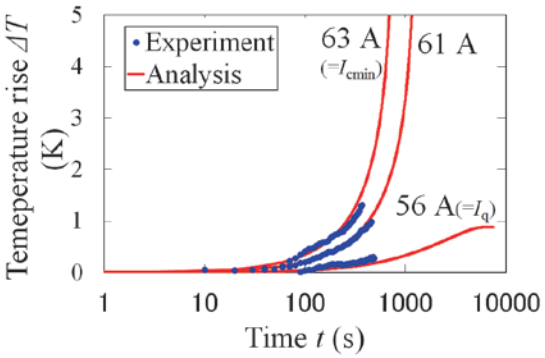

Figure 2. An example of the estimation of temperature rises of the HTS coil.

We also modeled screening currents I_s induced in HTS coils to investigate the effect of I_s on the coil magnetic field and a transport AC loss in an HTS coil for space applications of the HTS coil. We compared analysis results with experimental data obtained from the Bi-2223/Ag scale-down model coil. The experimental residual magnetization due to I_s in the Bi-2223/Ag coil can be effectively modeled assuming an equivalent loop length of approximate 9 mm for I_s in the coil. The values calculated from the method

quantitatively agreed with the results for various experimental conditions as well as the hysteresis of the magnetization due to I_s. These results demonstrated the validity of our model for screening currents I_s, which considers the effects of flux creep and smaller I_s loops in the multi-filamentary Bi-2223/Ag tape. The transport AC loss in an HTS coil under AC ripple currents with DC offsets was also investigated to use a DC/DC converter for space applications of the HTS coil. Our analysis clarified that larger DC offsets greatly increase the effective AC loss even under a smaller AC current. In addition, we showed that the AC loss decreased the thermal stability of the conduction-cooled coil in case that HTS tapes in the coil are in the flux-flow state such as the load factor of 80%. These results suggested that, in order to apply the AC ripple current to HTS coils, the operational load factor must be properly selected.

To design an optimal HTS coil for use in space, we analyzed the characteristics of HTS coils using a Bi-2223/Ag tape or YBCO coated-conductors. The suitable configuration of the HTS coil was searched within a diameter of 4 m to obtain a larger magnetic moment and clarify the obtainable propulsive force from the magneto plasma sail. We analyzed the current transport properties, thermal behavior, and applied stresses of the HTS coils, and compared these characteristics for each coil configuration. As a result of a sensitivity study, we showed that a thin-walled racetrack coil or multi-pole coil with YBCO coated-conductors could achieve the larger magnetic moment (as shown in Fig. 3) with allowable stresses and high thermal stability for space missions.

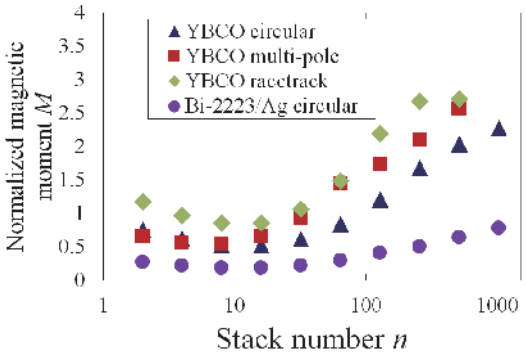

Figure 3. Dependence of the magnetic moment of the coils in the case of an outside radius of 2.0 m on the coil configuration.

The whole HTS coil system including the cooling system was also optimized to maximize the magnetic moment to mass ratio or acceleration, of the magneto plasma sail. The weight of the cooling system was considered for each coil configuration. We optimized the configuration of the coil using the genetic algorithm in the case of YBCO circular, multi-pole and racetrack coil at a variety of the operational temperatures from 10 K to 50 K on the condition of the perpendicular or parallel direction of the magnetic axis to the sun direction. Figure 4 shows the optimal coil system with the racetrack coil or multi-pole coil. For all kinds of the coils, the magnetic moment to mass ratio reaches the highest value at the operational temperature of around 20 K. On the other hand, in the case of using the HTS coil at less than 20 K, the magnetic moment to mass ratio rapidly decreases because a larger radiation cooling system is required. This study finally revealed that the racetrack coil system can maximize the magnetic moment to mass ratio of the system which is approximate three times larger than that of the minimum requirement for the magneto plasma sail.

The present study proved the possibility to increase the thrust to mass ratio of the magneto plasma sail greatly, and leads to realizing a space propulsion system using an HTS coil.

(a) Racetrack coil (b) Multi-pole coil

Figure 4. Overview of the optimal system of the magneto plasma sail with (a) racetrack coil or (b) multi-pole coil.

ABSTRACTS (MASTER THESIS)

Analysis of microwave effects in transesterification by lipase and oxidative degradation of lignin

(Graduate School of Agriculture, Laboratory of Biomass Conversion, RISH, Kyoto University)

Keigo Ito

Conversion of lignocellulosic biomass is emerging as one of the most important technologies for sustainable production of renewable fuels and chemicals due to its widespread availability, large quantity, non-competitiveness with food supply, potential as platform for green chemicals and high mitigation effects on GHG emissions. In conversion of lignocellulosic biomass, increase in conversion efficiency with low energy input is essential. Microwave heating is attractive for this purpose due to its rapid heating behavior toward the materials with high permittivity loss. In some chemical reactions, acceleration of reaction rate by microwave heating has been reported, and mechanisms for the phenomena have been discussed in terms of thermal and non-thermal effects. The effects observed in microwave-irradiated chemical transformations can in most cases be rationalized by purely bulk thermal phenomena associated with rapid heating to elevated temperatures[1], but other factors may affect the reaction efficiency. Thus, the mechanisms behind the acceleration, and in some cases changes in reaction selectivity, are not fully understood. In this research, effects of chain length of substrates on lipase-catalyzed transesterification between methyl methacrylate and aliphatic alcohols were analyzed to understand the factors affecting the reaction rate by microwave irradiation. Immobilized lipase was reacted in toluene with methyl methacrylate and aliphatic alcohols with different chain length (C6-C18) using conventional heating (CH) and microwave heating (MH) at 2.45 GHz using the same test tube by controlling the temperature profile to minimize the differences between CH and MH. A semiconductor amplifier was used to generate the microwave, and the temperatures in solutions were monitored using a fiber optic thermometer. Differential behavior in the reaction rate between CH and MH were observed, depending on the chain length of the alcohols used. This phenomenon was interpreted by applying an Arrhenius plot and transition state theory[2].

In addition to the enzymatic reaction, degradation of β-*O*-4 linin dimer model compound by copper complex and H_2O_2 were analyzed. When the reaction system was applied to wood particles, vanillin and vanillic acid were produced from softwood, and vanillin, vanillic acid, syringaldehyde and syringic acid were released from hardwood in a high yield comparable to that of nitrobenzene oxidation. MH gave these monomers by up to around two times higher yields than those of CH. Because the reaction toward wood involves multiple reactions including wood cell wall swelling, dissociation of the components, and oxidative lignin degradation, the accelerating effects of MH was not able to solely ascribe to the enhanced degradation of lignin substructures. This research aimed at elucidating if the MH affects directly on release of vanillin and vanillic acid by cleavage of Cα-Cβ bonds from a β-*O*-4 linin dimer model compound. The results showed that MH accelerated the degradation of lignin model compounds.

References

[1] Rosana, M. R., J. Hunt, A.Ferrari, T. A. Southworth, Y. Tao, A. E. Stiegman and G. B. Dudley, "Microwave-Specific Acceleration of a Friedel-Crafts Reaction: Evidence for Selective Heating in Homogeneous Solution", *J. Org. Chem.* 2014, 79, 7437-7450.

[2] Ito, K., H. Nishimura, T. Mitani and T. Watanabe, "Analysis of specific microwave effects in transesterification by lipase", *Abst. of the 66th Annual Meeting of the Japan Wood Res. Soc.*, 2016, Z27-08-1345.

ABSTRACTS (MASTER THESIS)

Microwave organosolvolysis with Lewis acid catalyst for biorefinery of sugarcane bagasse

(Graduate School of Agriculture, Laboratory of Biomass Conversion, RISH, Kyoto University)

Pannarai Khamdej

Global warming caused by emission of greenhouse gas by excessive use of fossil fuels, has promoted development of biofuels from renewable resources. Lignocellulosics is the most abundant renewable feedstock and it attracts considerable attention as new resources for production of biofuels and chemicals. One of the lignocellulosic materials found in great quantities, to be considered is sugarcane bagasse, although recalcitrance of the lignified plant cell wall structure is still a major limitation to utilize the plant materials. Pretreatment separating the cell wall polysaccharides, cellulose and hemicelluloses, from lignin is a crucial step to increase accessibility of polysaccharide hydrolases to their substrates prior to fermentation. In this study microwave-assisted organosovolysis with non-toxic food additive classified as Lewis acid was applied to disintegration of sugarcane bagasse for enzymatic saccharification and fermentation, and high efficiency of the process for bioethanol production was demonstrated.

Microwave pretreatment reaction of sugarcane bagasse was conducted in aqueous glycerol or 2-propanol in the presence of Lewis acid catalyst using a laboratory scale microwave reactor or a 1L microwave reactor designed for processing of biomass. After the pretreatment for 30 min, solid and liquid fractions were separated, then subjected to hydrolysis with cellulase. The reducing sugars released were determined by Somogi-Nelson method to evaluate the saccharification efficiency. Lignin content in the solid fraction was quantified. Efficiency of overall process was evaluated by separate hydrolysis and fermentation (SHF) in a test tube and simultaneous saccharification and fermentation (SSF) in a jar-fermenter using a gene-engineered ethanologenic bacterium *Zymomonas mobilis* strain capable of fermenting xylose and hexose sugars. Ethanol produced were analyzed by HPLC.

To optimize the reaction conditions, effects of 3 factors, water content, catalyst concentration and reaction temperature were evaluated in terms of the saccharification and delignification efficiency. The results showed that addition of Lewis acid in the microwave reaction considerably promoted removal of lignin from sugarcane bagasse, by 3-4 times higher efficiency than those without the catalyst. The pretreatment and enzymatic saccharification system was applied to a small scale SHF using recombinant *Z. mobilis* capable of utilizing xylose. Glucose was consumed in 24 hr with concomitant gradual decrease in xylose concentration. Bioethanol was produced in 97% of the theoretical yield. The pretreament system was scaled up to a 1L microwave reactor and SSF in a jar fermenter. The pretreatment was conducted at 180℃ in 70% glycerol with the Lewis acid catalyst at the concentration of 360 μmol/g dry biomass. After pre-hydrolysis for 48h, 78.6 g/L of glucose was released from 100 g of solid substrate, and ethanol yield reached 91% of the theoretical yield by SSF. The combination of microwave organosovolysis with Lewis acid catalyst showed promising results to utilize sugarcane bagasse as a substrate for bioethanol production toward commercial scale production.

ABSTRACTS (MASTER THESIS)

Analysis of interaction of 12-mer peptides and carbohydrate-binding module of cellulase with lignin

(Graduate School of Agriculture, Laboratory of Biomass Conversion, RISH, Kyoto University)

Takashi Suetomi

Lignin, a heterogeneous aromatic polymer provides plant cell walls structural rigidity and biological resistance. Lignin is the sole large-volume renewable feedstock composed of an aromatic skeleton. Highly selective degradation of lignin is pivotal for industrial production of paper, biofuels, chemicals, and materials. However, few studies have examined natural and synthetic molecular components recognizing the heterogeneous aromatic polymer. Recently lignin-binding 12-mer peptides were identified using a phage display technique[1]. The selected peptides were found to possess a characteristic sequence and exhibit structure-dependent high-affinity binding to the lignin isolated from softwood and hardwood. A consensus sequence was found in several lignin-binding peptides, but the outer amino acid sequence affected the binding affinity of the peptides. To characterize the key amino acid residues in the lignin-binding peptides, a peptide designated as C416 and its single-residue substituted peptides were subjected to the binding analysis with milled wood lignin (MWL) from softwood and hardwood by surface plasmon resonance. Substitution of the 7th residue of phenylalanine with isoleucine in the lignin-binding peptide (C416) decreased the affinity of the peptide for softwood lignin without changing its affinity for hardwood lignin, indicating that the peptide recognized structural differences between the lignin. Circular dichroism spectroscopy demonstrated that C416 adopted a highly flexible random coil structure, allowing key residues to be appropriately arranged in relation to the binding site in lignin. In this study binding of the lignin-binding peptides with β-*O*-4 lignin dimer and oligomer model compounds and also with milled wood lignin (MWL) was studied using NMR. Spectral changes were found on addition of these lignin model compounds and isolated lignin depending on concentration of the additives, and the results were interpreted based on the structures of the peptide sequence. In this study carbohydrate-binding module (MWL) of cellobiohydrolase were expressed in *Pichia pastoris*, and binding to the MWL was analyzed using NMR. Differences were found for the binding behavior between cellohexaose and MWL. These binding analysis provides a useful platform for designing synthetic and biological catalysts selectively bind to lignin. Analysis of the binding between peptides/CBM and lignin would also give important information to unveil the molecular interaction between polysaccharide hydrolases and lignin, which is a key factor to suppress unproductive binding of the enzymes with lignin during enzymatic saccharification of lignocellulosic biomass for production of biofuels and chemicals.

Reference

[1] Yamaguchi, A., K. Isozaki, M. Nakamura, H. Takaya, T. Watanabe, Discovery of 12-mer peptides that bind to wood lignin, *Scientific Reports*, 6, 21833, 2016.

ABSTRACTS (MASTER THESIS)

Characterization of lignocellulose in fractionated stem tissues of large-sized Gramineae biomass crops

(Graduate School of Agriculture, Laboratory of Metabolic Science of Forest Plants and Microorganisms, RISH, Kyoto University)

Akihiro Hayashi

The genus *Erianthus*, a group of large-sized Gramineae plants, belongs to the Saccharainae subtribe within tribe Andropogoneae in the Gramineae family and is part of the *Saccharum* complex. *Erianthus* has various agriculturally important traits such as a high productivity, ratooning ability, rapidity of growth, and resistance to environmental stresses, and has been considered potentially as an important genetic resource for breeding of *Saccharum*. The dry-matter yields of biomass amounts in *Erianthus* are 40-60 ton ha^{-1} $year^{-1}$ in Japan and USA [1, 2], and these yields are higher than those of miscanthus and swichgrass.

Despite of the fact that *Erianthus* is receiving much attention as potential biofuel and industrial feedstocks, there has been only limited information regarding the lignocellulosic compositions and enzymatic saccharification for producing bioethanol. Recently, Yamamura et al. characterized lignocellulose in several organs of *Erianthus arundinaceus* Type I [3, 4] in terms of lignins and enzymatic saccharification efficiencies, and found that the outer part (rind) of the internode showed a negative correlation between lignin contents and enzymatic saccharification efficiencies, whereas there was no clear correlation in the inner part (pith). The result suggests that not only lignin content but also other factors simultaneously influence the enzymatic saccharification efficiency of the pith of *E. arundinaceus* [4].

In this study, to further investigate the relationship between lignocellulose structures and enzymatic saccharification efficiency, lignocelluloses of stem tissue fractions in two *E. arundinaceus* genotypes, Type-I and IJ76-349, and *Sorghum bicolor* SE1 were characterized using various chemical analyses and 2D-NMR analysis, and obtained structural data were compared in relation to the enzymatic saccharification efficiency. Lignin content and composition as well as cell wall-bound *p*-coumarate content varied among fractionated tissues, and also among the plant species, whereas characteristics of cellulose and hemicelluloses were all similar. Correlation analysis showed that enzymatic saccharification efficiency is well correlated with both lignin content and composition in *S. bicolor*, whereas there was no or weak correlation in both the two *E. arundinaceus* genotypes, suggesting that enzymatic saccharification efficiency of *Erianthus* was negatively affected not only by lignin content but also by other factors such as supramolecular structure of lignocellulose. Our data collectively suggest that structure and assembly of cell wall lignins in large-sized Gramineae plants considerably vary among the species and substantially impact the enzymatic conversion of lignocelluloses to bioethanol.

References

[1] Takahashi W, Takamizo T “Molecular breeding of grasses by transgenic approaches for biofuel production” In: Çiftçi YO (ed) Transgenic plants—advances and limitations. InTech, Rijeka, pp 91-116, 2012.

[2] Mislevy P, Martin FG, Adjei MB, Miller JD “Harvest management effects on quantity and quality of Erianthus plant morphological components.” Biomass and Bioenergy 13, 51-58,1997.

[3] Tagane S, Ponragdee W, Sansayawichai T, Sugimoto A, Terajima Y. “Characterization and taxonomical note about Thai *Erianthus* germplasm collection: the morphology, flowering phenology and biogeography amond *E. procerus* and three types of *E. arundinaceus*” Genetic Resources and Crop Evolution 59, 769-781, 2012

[4] Yamamura M, Noda S, Hattori T, Shino A, Kikuchi J, Takabe K, Tagane S, Gau M, Uwatoko N, Mii M, Suzuki S, Shibata D, Umezawa T. “Characterization of lignocellulose of *Erianthus arundinaceus* in relation to enzymatic saccharification efficiency.” *Plant Biotechnol* **30**, 25-35, 2013.

ABSTRACTS (MASTER THESIS)

Structural modification of rice lignin by regulating aromatic hydroxylase gene expressions

(Graduate School of Agriculture, Laboratory of Metabolic Science of Forest Plants and Microorganisms, RISH, Kyoto University)

Yuri Takeda

Lignocellulose, a promising resource for productions of biofuels and bio-based materials, is majorly composed of three different polymers, i.e., cellulose, hemicelluloses, and lignin. While numerous technologies that transform biomass polysaccharides (cellulose and hemicelluloses) to bioethanol and various materials are becoming mature, cost-effective utilization of lignin has been substantially more challenging, representing one of the major issues that are to be overcome for establishing an economically feasible biorefinery system. In this context, our laboratory has been studying metabolic engineering of lignin to upgrade biomass feedstocks for biorefinery. Our study focuses on lignin bioengineering using a grass model plant, rice (*Oryza sativa*), in particular to obtain fundamental knowledge for improving the properties of grass biomass crops, e.g., swichgrass, *Erianthus*, and *Miscanthus*, that are expected as a potent biomass resource especially because of their high biomass productivity [1-3].

Lignin is mainly composed of three different types of aromatic component, guaiacyl (G), syringyl (S), and *p*-hydroxyphenyl (H) units. Lignin composition, i.e., G/S/H lignin unit ratio, has been identified as an important structural trait that impacts usability of lignin and also lignocellulose as a whole. In the lignin biosynthetic pathway in angiosperms, ferulate 5-hydroxylase (F5H) and *p*-coumaroyl ester 3-hydroxylase (C3´H) have been identified as the major enzymes that modulate aromatic ring structures of lignin monomer units. In this study, we identified major genes encoding F5H and C3´H functioning in the deposition of lignin in rice, and demonstrated that modulation of their expressions led to substantial alterations in G/S/H lignin unit ratio of rice cell walls.

Based on our analyses on protein sequence and gene expression, we determined major rice F5H (*OsF5H1*) and C3´H (*OsC3H1*) genes that are homologous to the previously-characterized F5H and C3´H enzymes in dicots, and they are predominantly expressed in lignin-producing rice organs. We then generated transgenic rice plants in which *OsF5H1* or *OsC3H1* is up- or down-regulated, and characterized their cell wall chemotypes using wet-chemical and 2D NMR approaches. As expected, down- and up-regulation of *OsF5H1* produced altered lignins largely enriched in G and S units, respectively, and down-regulation of *OsC3H1* resulted in lignins considerably enriched in H units. In addition, down-regulation of *OsC3H1* also led a substantial decrease in wall-bound ferulates, cross-linkers between lignin and polysaccharide and one of the unique structural traits of grass lignocellulose. Our data collectively demonstrate that *OsF5H1* and *OsC3H1* are primary genes controlling G/S/H lignin composition in rice cell walls. Overall, we contemplate that manipulation of F5H and C3´H gene expressions could be a promising strategy to upgrade grass lignocellulose for future biorefinery.

References

[1] Hattori T., Murakami S., Mukai M., Yamada T., Hirochika H., Ike M., Tokuyasu K., Suzuki S., Sakamoto M., and Umezawa T. “Rapid analysis of transgenic rice straw using near-infrared spectroscopy.” *Plant Biotechnol.* 29, 359-366, 2012.

[2] Koshiba T., Hirose N., Mukai M., Yamamura M., Hattori T., Suzuki S., Sakamoto M., and Umezawa T. “Characterization of 5-Hydroxyconiferaldehyde *O*-Methyltransferase in *Oryza sativa*.” *Plant Biotechnol*. 30, 157-167, 2013.

[3] Yamamura M, Noda S, Hattori T, Shino A, Kikuchi J, Takabe K, Tagane S, Gau M, Uwatoko N, Mii M, Suzuki S, Shibata D, Umezawa T. “Characterization of lignocellulose of *Erianthus arundinaceus* in relation to enzymatic saccharification efficiency.” *Plant Biotechnol* **30**, 25-35, 2013.

ABSTRACTS (MASTER THESIS)

Functional analysis of flavonoid substrate prenyltransferase from *Macaranga tanarius*

**(Graduate School of Agriculture,
Laboratory of Plant Gene Expression, RISH, Kyoto University)**

Yoshiaki Date

Prenylation reaction of polyphenolic compounds largely contributes to the chemical and biological diversities in secondary metabolism of plants. To date, ca. 1,000 prenylated aromatic compounds were identified from a variety of plant species, and many of those secondary metabolites exhibit useful biological activities like antimicrobial and anti-tumor activities. Prenyltransferase (PT) plays a critical role in the biosynthesis of those prenylated compounds, whereas only a few PTs have been isolated until now. Glandular trichomes of *Macaranga tanarius* (*Euphorbiaceae*) are known as the plant origin of Okinawan propolis, which contains a large amount of prenylated flavonoids [1,2] ; however no PTs from *Euphorbiaceae* have been reported so far. On those background we tried to isolate *M. tanarius* PTs (MtPTs), and analyze their biochemical functions in this study.

We isolated candidate clones, *MtPT1* and *MtPT3*, and thier full-length sequences were subcloned into a binary vector to make *MtPTs* expression constructs in a plant host. Then, *MtPTs* were transiently expressed in *Nicotiana benthamiana* leaves by using agroinfiltration method. Microsome fractions of the leaves were prepared as crude enzymes for prenyltransferase assay, and their enzymatic function was analyzed. As results, MtPT1 catalyzed prenylation of a flavanone substrate to give prenylated flavonoids. Besides, MtPT3 also showed prenylation activity to a flavanone. We then analyzed the subcellular localization of MtPT1 and MtPT3 by using N-terminal regions of each enzymes fused to GFP respectively. In addition, we investigated *M. tanarius* organ-specific expression of *MtPT1* by real time PCR. MtPT1 and MtPT3 are the first PTs isolated from the family *Euphorbiaceae*. We expect that these PTs being contributed to progression of molecular evolution of PT superfamily, and also metabolic engineering for industrial production of natural medicinal compounds.

Acknowledgements

We thank Dr. T. Nakagawa (Shimane University), Dr. H. Kochi (International Christian University) and Dr. T. Mitsui (Niigata University) for the vectors, Dr. K. Miyagi (Okinawa Prefecture Forest Resources Research Center) and Dr. S. Fukumoto (Pokka Sapporo Food & Beverage Ltd.) for *M. tanarius* Samples, Dr. T. Kuzuyama (The University of Tokyo), Dr. T. Kawasaki (Ritsumeikan University), Dr. H. Yamamoto (Toyo University) and Dr. S. Kumazawa (University of Shizuoka) for chemical compounds used in enzyme assay.

References

[1] Kumazawa S., Nakamura J., Murase M., Miyagawa M., Ahn M. R., Fukumoto S., Plant origin of Okinawan propolis: honeybee behavior observation and phytochemical analysis. *Naturwissenschaften* 95: 781–786, 2008.

[2] Kumazawa, S., Goto, H., Hamasaka, T., Fukumoto, S., Fujimoto, T., Nakayama, T., A new prenylated flavonoid from propolis collected in Okinawa, Japan. *Bioscience, Biotechnology, and Biochemistry* 68 (1): 260-262, 2004.

[3] Sasaki, K., Mito, K., Ohara, K., Yamamoto, H., Yazaki, K., Cloning and characterization of naringenin 8-prenyltransferase, a flavonoid-specific prenyltransferase of *Sophora flavescens*. *Plant Physiology* 146 (3): 1075-1084, 2008.

ABSTRACTS (MASTER THESIS)

Proteome analysis of a shikonin-producing medicinal plant *Lithospermum erythrorhizon*

**(Graduate School of Agriculture,
Laboratory of Plant Gene Expression, RISH, Kyoto University)**

Yukimi Nakagawa

A herbal medicinal plant *Lithospermum erythrorhizon* Sieb. et Zucc. produces characteristic red naphthoquinone pigments, shikonin deriveatives in the root bark (Fig. 1). In this perennial plant, shikonin exists as ester derivatives, among which acetyl ester is the majority. These compounds exhibit a variety of biological activities, such as antibacterial and antivirus activities, as well as hemostatic activity. In fact, *L. erythrorhizon* has been used as a traditional medicine for over thousand years, and also as dyes for purple color.

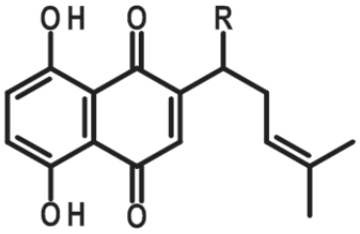

Compound	R
Deoxyshikonin	−H
Shikonin	−OH
Acetylshikonin	−OCOCH3
Isobutylshikonin	−OCOCH(CH3)2
β-Hydroxy -isovalerylshikonin	−OCOCH2C(OH)−(CH3)2

Fig. 1. Shikonin derivatives in *L. erythrorhizon*

Cell suspension cultures of this plant capable of producing a large amount of shikonin derivatives were established in 1970s, which was then utilized for industrial production of shikonin after establishment of a successful shikonin production medium M9 in 1980s [1] [2]. In the biosynthetic rout, shikonin is biosynthesized from *m*-geranyl-*p*-hydroxybenzoic acid (GBA), which is generated via coupling reaction of geranyl diphosphate provided from mevalonate pathway and *p*-hydroxybenzoic acid from phenylpropanoid pathway. The biosynthetic pathway from GBA to shikonin, namely how naphthoquinone skeleton is formed, is however still largely unknown.

In order to identify proteins involved in shikonin biosynthesis, we have in this study performed a comparative proteome analysis using the cultured *L. erythrorhizon* cells under the conditions with or without induction of shikonin biosynthesis. As the results, we obtained more than three thousand protein sequencess, from which ca. six hundred proteins specifically expressed only in shikonin-producing cells were picked up. We found several new enzymes including known enzymes involved in shikonin biosynthesis in the list. We will further use those candidates of the shikonin biosynthetic enzymes for the functional analysis in future.

References

[1] Fujita, Y., Tabata, M., Nishi, A., Yamada Y., New medium and production of secondary compounds with the two-stage culture method. In: Plant Tissue Culture 1982. Fujiwara A (ed), pp. 312-313. Maruzen, 1982.

[2] Fujita, Y., Hara, Y., Suga, C., and Morimoto, T., Production of shikonin derivatives by cell suspension cultures of *Lithospermum erythrorhizon*. 2. A new medium for the production of shikonin deivatives. *Plant Cell Rep.* 1: 61-63, 1981.

ABSTRACTS (MASTER THESIS)

Phylogeny and host specificity of rhizobia from Japanese alpine legume

**(Graduate School of Agriculture,
Laboratory of Plant Gene Expression, RISH, Kyoto University)**

Naoto Seo

Legume plants are living in association with rhizobia, which fix atmospheric nitrogen into ammonia that is provided to the host legumes as nitrogen nutrients (symbiotic nitrogen fixation). Legume plants can therefore grow under severe environments, such as in high mountain areas, while it is potentially accompanied by the risk that non-cooperative bacteria invade the host plant body. To avoid the risks, they developed host specificity. The determinant of the host specificity is investigated to some extent, but it is far from the comprehensive understanding. For this aspect, Japanese alpine flora is estimated to have been formed by relics of the plants that went south from the Arctic Circle during the quaternary cold periods [1]. In this point, Japanese alpine plants are suitable for an evolutionary study, and, in fact, some of Japanese alpine plants have been analyzed by phylogeographycal methods.

In this study, we have analyzed Japanese alpine legumes and their symbionts, in order to gain an insight into the change of host specificity that happened on a scale for tens of thousands years. First, we gathered two species of Fabaceae, i.e., *Hedysarum vicioides* and *Oxytropis japonica*, from 5 Japanese alpine regions, and isolated their symbionts from their root nodules. Analysis of the sequences of 16S rRNA genes of the symbionts was performed to identify the genus of them. As a result, they are found to belong to *Mesorhizobium, Burkholderia* and *Paenibacillus* etc. Among them, representative *Mesorhizobium* strains were found to be new species.

We performed then the network analysis of housekeeping genes and symbiotic genes of these rhizobia. As for housekeeping genes, a variety of allele was recognized, while symbiotic genes were conserved every host plant species regardless of the genus of symbionts. This result implies two possibilities on the transition of host specificity of legume-rhizobia symbiosis. One possibility is that legumes and rhizobia have been segregated to Japanese alpine areas maintaining the symbiosis. Another one is that after the segregation, the symbiotic genes of the original symbionts have spread to indigenous bacteria in the alpine area. In fact, the latter case was reported in the previous study [2]. These possibilities are partially supported by the rhizobia inoculation test. In order to perform phylogeographic analysis of Japanese alpine legumes, we have thus developed SSR (Simple Sequence Repeat) markers. Using these markers, it is expected to perform phylogeographic analysis and association with host specificity.

Acknowledgements

This study was supported by Dr. H. Nishimura of RISH, Kyoto University; Dr. S. Sato of Graduate School of Life Sciences, Tohoku University; Dr. H. Hirakawa and Dr. Y. Nakajima of Kazusa DNA Res. Inst.

References

[1] Toyokuni, H., A preliminary note on the floristic phytogeography of the alpine flora of Japan, *J Fac Lib Arts Shinshu Univ Nat Sci*, 15:81-96, 1981.

[2] Lemaire, B., Van Cauwenberghe, J., Chimphango, S., Stirton, C., Honnay, O., Smets, E., Muasya, A. M., Recombination and horizontal transfer of nodulation and ACC deaminase (acdS) genes within Alpha- and Betaproteobacteria nodulating legumes of the Cape Fynbos biome. *FEMS Microbiol Ecol.*, 91(11): pii: fiv118, 2015.

ABSTRACTS (MASTER THESIS)

Analysis of root contents, secretion and degradation dynamics of isoflavonoids in soybean

**(Graduate School of Agriculture,
Laboratory of Plant Gene Expression, RISH, Kyoto University)**

Yumi Yamazaki

Isoflavonoids secreted from soybean roots function as an essential signal molecule for the symbiosis with rhizobia. Isoflavonoids have been also shown to be involved in the interactions with arbuscular-mycorrhizal fungi and pathogens in the rhizosphere [1]. Because most functions of isoflavonoid were examined using plants grown in hydroponic cultures or under controlled environments containing solely a single microbe of interest, the actual functions of isoflavonoids in rhizosphere, especially in field condition still remain to be elucidated.

In this study, we have focused on the roles of isoflavonoids in soybean rhizosphere, and analyzed isoflavonoid contents in each plant tissues and secretion from roots, as well as the degradation dynamics of isoflavonoids in soil. We also analyzed the expression of *ICHG* (Isoflavone Conjugate-Hydrolyzing β-Glucosidase) in soybeans grown in hydroponic culture and also in the field. In hydroponic culture condition, HPLC analysis showed that the contents and composition of isoflavonoids in leaves and roots were not dynamically altered during development, while those in root exudates clearly differed, depending on the developmental stages. Daidzein was the predominant form of isoflavonoids in the root exudates of soybeans, especially at vegetative stages. The amount of malonyldaidzin was increasing at reproductive stages. Moreover, analysis of *ICHG* expression by real-time PCR showed that *ICHG* expression was higher at vegetative phases during soybean development, but was reduced during reproductive stages. This was in line with the data on the isoflavonoid secretion [2]. As for field studies, we planted soybeans (Glycine max cv. Shin-Tambaguro) in the field at Kyoto Gakuen University, and sampled the leaves and roots at 2, 5, 8, 11, 15, 20 weeks after germination. In the field condition, the contents and composition of isoflavonoids in leaves and roots were not dynamically altered during development, which is same as in hydroponic culture condition. *ICHG* expression was higher at vegetative stages and was reduced during reproductive stages, suggesting that the *ICHG*-mediated pathway for the isoflavonoid secretion has an important role at vegetative stages also in filed. The extraction of isoflavonoids from rhizosphere and bulk soil showed that daidzein was dominant form of isoflavonoids in soil, with more than 100-fold abundance in the rhizosphere. In the degradation analysis, daidzein was shown to be degraded within 3 weeks in both rhizosphere and bulk soils.

Acknowledgements

We would like to thank Dr. Hisabumi Takase for supporting and offering the experimental field. We thank Dr. Toru Nakayama and Dr. Seiji Takahashi for providing the primer sequences of *ICHG*. We are also grateful to Ms. Yuko Kobayashi and Dr. Saya Shirai for technical assistance. This study was partly supported by DASH/FBAS of Research Institute for Sustainable Humanosphere, Kyoto University, and a grant from the Ministry of Agriculture, Forestry, and Fisheries of Japan (Genomics-based Technology for Agricultural Improvement, SFC2001).

References

[1] Sugiyama, A., Yazaki, K., “Root exudates of Legume Plants and Their Involvement in Interactions with Soil Microbes”, *Secretions and Exudates in Biological Systems*, 12: 27-48, 2012.

[2] Sugiyama, A., Yamazaki, Y., Yamashita, K., Takahashi, S., Nakayama, T., Yazaki, K., “Developmental and nutritional regulation of isoflavone secretion from soybean roots”, *Bioscience, Biotechnology, and Biochemistry*, 80 (1): 89-94, 2016.

ABSTRACTS (MASTER THESIS)

A study on an ultraviolet rotational Raman lidar for temperature profiling with a multispectral detector

(Graduate School of Informatics, Laboratory of Atmospheric Sensing and Diagnosis, RISH, Kyoto University)

Yoshikazu Okatani

Temperature profiling in the atmosphere is essential in meteorological studies for understanding atmospheric processes. Rotational Raman (RR) lidar can be used to observe temperature based on the intensities of the lines within the RR band that exhibit different dependencies on temperature. In this study, we constructed a temperature lidar with a multispectral detector (MSD) using an ultraviolet (UV) laser. We validated the calibration methods of the lidar system and estimated the errors caused by the analytical methods and atmospheric conditions.

Two methods were investigated to correct the MSD efficiency of each channel: 1) comparison of lidar signals with temperature profiles of radiosonde to determine the calibration factors; 2) calibration of the MSD efficiency by standard calibration lamp technique. Our findings show that, although the calibration values of the radiosonde method were strongly affected by the detector wavelength resolution and laser wavelength, the values of the calibration lamp method could be determined independently of the lidar system. The maximum difference in the calibration values between the two methods was 1.3% for the four channels, except for when leakage effect caused by strong elastic scattering in the detector.

Atmospheric temperature can be estimated by fitting the corrected lidar signals to the theoretical Raman spectrum. We have evaluated the suitable fitting methods for temperature estimation of the UV Raman lidar, and calculated the temperature from the lidar signals at a laser wavelength of 355 nm with the applied correction of the two calibration methods. The derived temperature displayed similar trends for the two methods and the differences of the temperature by comparison with radiosonde at the heights of 1850-2150 m and 2150-2450 m were 0.05-0.6 K and 3.1-7.0 K, respectively.

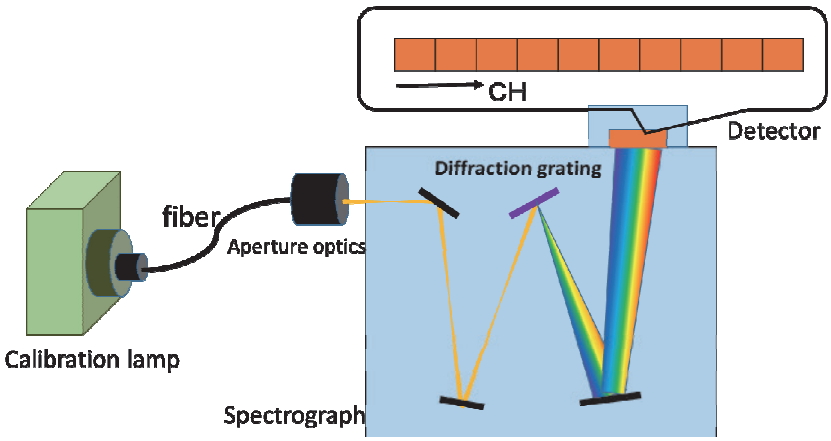

Figure 1. Schematics of the calibration setting of a temperature lidar with a multispectral detector by standard calibration lamp technique.

ABSTRACTS (MASTER THESIS)

An observational study on the real-time precipitable water vapor with a dense GNSS receiver network

**(Graduate School of Informatics,
Laboratory of Atmospheric Sensing and Diagnosis, RISH, Kyoto University)**

Yuji Takeda

We aim to observe the behavior of water vapor during a rainfall. We employ the GNSS meteorology to estimate a vertically integrated water vapor, so called PWV (Precipitable Water Vapor), from the propagation delay of GNSS signal. We established a dense GNSS receiver network in Uji using 15 receivers with 1-2 km spacing. We found difference of PWV in 10 km was 3-10 mm during a heavy rain. For a future GNSS network in a much wide area, we use inexpensive single-frequency (SF) receivers. Because SF receiver cannot eliminate the ionospheric delay, we interpolate the delay referring to the results from nearby dual frequency (DF) receivers.

We investigated ionospheric delay by the Uji network, taking advantages of QZSS (Quasi-Zenith Satellite System) that gives signals at high elevation angles. Effects of ionospheric perturbations due to sun-rise/sun-set and a geomagnetic storm were small, so they do not give serious influence on PWV. During a travelling ionospheric disturbance, a wavy structure with a horizontal scale of several tens km was recognized. These ionospheric effects can be compensated by a linear or quadratic interpolation.We corrected the ionospheric delay on SF observation with 30 sec sampling with SEID developed by GFZ (see Fig.1). The resulting error of PWV compared with DF solution was about 1.50 mm in RMS.

For a real-time estimating of PWV, we need to know accurate satellite orbit and clock products, which are calculated from real-time satellite clock information corrected by GEONET. Difference of PWV between the real-time analysis and the post processing by using the final orbit information was 0.68 mm in RMS.

In summary, we estimate overall error of PWV with a dense SF-receiver network on a real-time basis is 1.65 mm in RMS, which is accurate enough to depict the horizontal variations of PWV during a severe rainfall event. We hope our study will contribute to an early warning system for weather hazards.

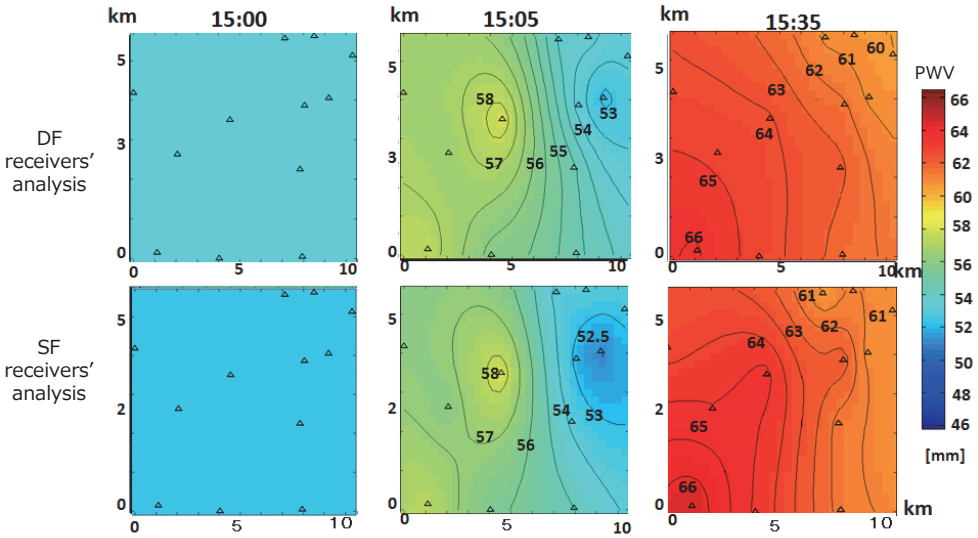

Figure 1. The horizontal distributions of precipitable water vapor (PWV) observed from a dense GNSS receiver network in Uji with the dual frequency analysis (upper panels) and the single frequency analysis (lower panels) on August 3, 2012.

ABSTRACTS (MASTER THESIS)

Characteristics of dynamical and chemical fields in Chemistry Climate Models

(Graduate School of Science, Laboratory of Atmospheric Environmental Information Analysis, RISH, Kyoto University)

Takuya Sasaki

We analyzed results from three coupled chemistry-climate models (CCM) to investigate characteristics of climatological differences between free-running (FR) and specified dynamics (SD) modes, by paying attention to interactions between dynamical and chemical fields. The three models used in this study are the NCAR Whole Atmosphere Community Climate Model, version 4 (WACCM4) (Marsh et al., 2013), the Model for Interdisciplinary Research on Climate 3.2 Chemistry Climate Model (MIROC3.2-CCM) (Imai et al., 2013; Sakazaki et al., 2013), and the Meteorological Research Institute Earth System Model Version 1 Revision 1 (MRI-ESM1r1) (Deushi and Shibata, 2011; Adachi et al., 2013). Outputs from the three models are based on simulations proposed by IGAC/SPARC Chemistry Climate Model Initiative (CCMI) to improve our understanding in modelling of the chemistry and dynamics of the troposphere and stratosphere. Simulations have been conducted for the period of 1980-2010 as monthly means.

We carefully analyzed differences found at mid-high latitudes in the stratosphere of the winter hemisphere, the extratropical upper troposphere and lower stratosphere (Ex-UTLS) and the tropical tropopause layer (TTL). Comparisons of stratospheric temperatures at mid-high latitudes show that for all FR-CCM results the seasonal change is delayed in both hemispheres during the winter and spring; especially in the southern hemisphere all FR-CCM results show cold biases in early spring. Results for ozone are similar to those for temperature, and the biases in the southern hemisphere are clearer than in the northern hemisphere. We also investigated the Eliassen-Palm fluxes (EP flux) and resulting residual mean meridional circulations, because the seasonal changes in temperature and ozone during these seasons and in those regions are affected by the meridional circulation. EP flux convergences and downward velocities in winter are smaller for all FR-CCM results than SD-CCM ones, indicating that the time of maximum wave activities seen in EP fluxes are delayed about 1-2 months for all FR-CCM results. These suggest that the temperature and ozone biases are due to some problems with model reproducibility of planetary waves propagating into the stratosphere from the troposphere.

In the Ex-UTLS, all FR-CCM results show cold biases especially in summer, and all SD-CCM results overestimate radiative cooling effects. Comparisons of water vapor with satellite observations (Aura-MLS) and models show that all model results overestimate water vapor in the upper troposphere at mid-high latitudes. Because water vapor has an important role in the radiation budget during the summer in this region, the FR-CCM cold biases and the SD-CCM overestimations of radiative effects are from water vapor overestimations. The dynamical fields are specified in SD-CCM, therefore these overestimations are due to the model reproducibility of chemical, transport and microphysics processes associated with water.

In the TTL, we compared ozone distributions in SD-CCM and FR-CCM results. We found that FR-CCM of MIROC3.2-CCM and WACCM4 cannot reproduce the increase of ozone in boreal summer. This is due to the annual cycle of upwelling and the horizontal transport from mid latitude; this mechanism is called in-mixing and is understood as the nearly isentropic transport owing to the Asian and North American monsoon anticyclones. WACCM4 FR-CCM can reproduce this increase in isentropic coordinate, and the Asian monsoon anticyclone is weak in the FR-CCM of MIROC3.2-CCM. These indicate that temperature and monsoon anticyclone reproducibility is strongly related to the improvement of ozone results in the TTL.

ABSTRACTS (MASTER THESIS)

Development of MU radar real-time processing system with adaptive clutter rejection

**(Graduate School of Informatics,
Laboratory of Radar Atmospheric Science, RISH, Kyoto University)**

Takahiro Manjo

Strong clutter echoes from a hard target such as a mountain or building sometimes cause problems of observations with atmospheric radars (Figure 1). In order to reject or suppress clutter echoes, it is effective to use NC-DCMP (Norm Constrained-Directionally Constrained Minimum Power) method, which makes null toward the direction of the clutter, if we can receive signals independently from plural antennas. The MU (Middle and Upper atmosphere) radar which located in Shigaraki, Shiga Prefecture, Japan is one of the most powerful VHF-band atmospheric radars, which can observe atmospheric motion and circulation between the troposphere and the upper atmosphere and which has contributed to a wide variety of research areas. Its operational frequency, occupied frequency bandwidth, and peak output power are 46.5 MHz, 3.5 MHz and 1 MW, respectively. The MU radar has an active phased array system. Its antenna consists of 475 elements of crossed Yagi antennas and is divided into 25 groups. Each group has 19 antenna elements. After installing the ultra multi-channel digital receiving system in 2004, we can receive signals from each 25 group, independently. It has been demonstrated that the NC-DCMP method is effective to real observation data with the MU radar, but it was processed in off-line [1].

The objective of this study is to implement the clutter rejection by NC-DCMP method into the on-line processing system of the MU radar. Namely, we can adaptively suppress clutter echoes in real time without changing any MU radar hardware and can reduce volume of data so that we can continue observation for a long time without taking care of storage capacity. Moreover, applying NC-DCMP method enables us to estimate velocity of the vertical wind more accurate. When we use NC-DCMP method, we need to determine a value of Norm-Constrain. The optimize value of it will change depending on the environment of the clutter. In this study, we discussed it and the way how we introduce this method into the existing system optimally and smoothly. Then we practiced it and have made sure that it works in real-time. Through the discussing and analyzing the data we have got, it is suggested that higher mountains exist in the almost same range where we receive strong clutter echoes and that the environment of the clutter will change depending on distribution of temperature. We can apply the achievement of this study to the Equatorial MU radar (EMU), which is proposed to be constructed at West Sumatera, Indonesia. The EMU system is the similar as the MU radar, but its antenna consists of 1045 Yagi antennas with 55 groups.

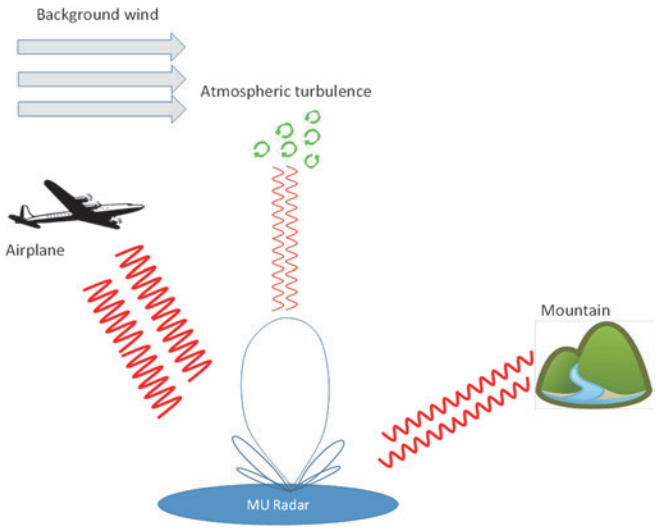

Figure 1. Clutter echoes from mountain, airplane etc. are received with antenna sidelobe, while atmospheric echoes with mainlobe.

Reference

[1] Nishimura, K., T. Nakamura, T. Sato, and K. Sato, "Adaptive Beamforming Technique for Accurate Vertical Wind Measurements with Multichannel MST Radar," *J. Atmos. Ocean. Tech.*, 29, 1769-1775, 2012.

ABSTRACTS (MASTER THESIS)

Development of real-time three dimensional analysis system of the ionosphere over Japan based on GPS-TEC observations

**(Graduate School of Informatics,
Laboratory of Radar Atmospheric Science, RISH, Kyoto University)**

Shota Suzuki

Real-time information of the ionospheric electron distribution is important for the correction of the measurement errors in satellite navigation. It is hoped that tsunami warning systems may be realized if such real-time monitoring of ionospheric disturbances is available. In this study, we developed three-dimensional ionosphere tomographic analysis based on the GPS-TEC data from 200 stations over Japan (Figure 1) and the tomography analysis technique proposed by Gopi *et al*. [1]. As the GPS-TEC data are available at every second, we constructed a software system for the real-time monitoring of the ionosphere over Japan.

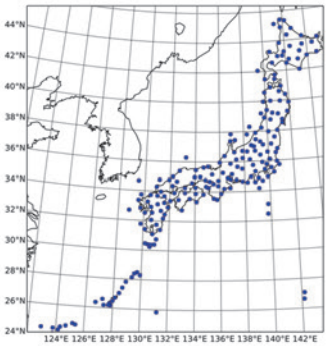

Figure 1. Distribution of 200 GPS stations where 1s data are available.

The developed system consists of four parallel processes; parallel decoding of BINEX binary data, estimation of instrument bias, two-dimensional fluctuated and absolute TEC distribution analyses and the three-dimensional tomographic analysis.

The instrument biases are calculated in parallel by using the previous 24 hour data. By adapting an algorithm of sparse matrix for matrix operations, the computation time was reduced from about two hours to less than one second, which makes it possible to update the instrumental biases every hour. And the estimation error of instrumental biases was reduced by this way.

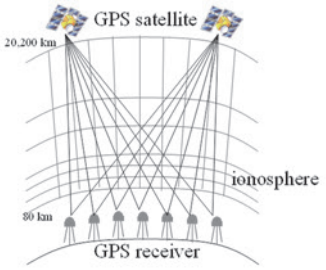

Figure 2. Conceptual figure of the ionospheric tomography.

In the three-dimensional tomographic analysis (Figure 2), calculation time of the tomographic matrix was reduced to less than 10 minutes by adapting the algorithm of spline interpolation and sparse matrix operations. It is about three times faster than the previous program. L-curve method was adopted for determining hyper parameter of the evaluation function. Boundary conditions are applied to three-dimensional grids. Because of these changes, now we can obtain stable solutions within about 10 minutes after the measurement by GEONET 200 stations. Figure 3 shows an example of meridional-height section of the plasma density obtained from the tomography analysis. The results show good agreement with other observations from the GPS occultation and ionosondes.

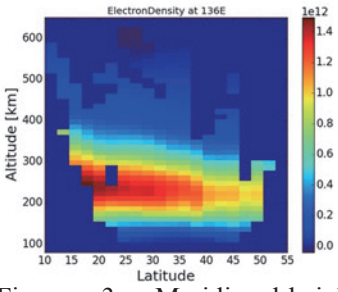

Figure 3. Meridional-height section of the plasma density from 3D tomography at 7:00UT on May 23, 2012.

The real-time tomography system started its service in April 2016 at Electronic Navigation Research Institute (ENRI). Now the 3D ionospheric plasma density is available at every 15 minutes with about 10 minutes latency from the following URL.

http://www.enri.go.jp/cnspub/tomo3/

Reference

[1] Seemala, G. K., Yamamoto, M., Saito, A. and Chen, C.-H.: Three-dimensional GPS ionospheric tomography over Japan using constrained least squares, *J. Geophys. Res. Space Phys.*, **119**, 3044-3052, 2014.

ABSTRACTS (MASTER THESIS)

Study on the extreme weather mechanism of urban area by combining a Doppler lidar and high-resolution numerical model

**(Graduate School of Informatics,
Laboratory of Radar Atmospheric Science, RISH, Kyoto University)**

Kenya Yano

In the summer season, the disastrous severe rain frequently occurs by Global warming in Japan. The small-scale convergence of humidity in the boundary layer is considered as one of the most important factor to determine the generation of such a disastrous rainstorm. The wind condition near the surface of the ground is affected by the ground condition so we cannot get the detailed information by direct observation. It is very difficult to capture the urban wind condition in complex surface.

In this study, to get the wind condition of the lower atmosphere, we successfully started observations using a coherent Doppler lidar (CDL) in May 26, 2015. CDL can observe air convergence of first stage because observing object is not raindrop but aerosol. We got the presence of wind strength in a small scale because the data of CDL is a 100-m resolution (Fig.1 (a)).

Using model is WRF (Weather Research and Forecasting) model which is non-hydrostatic weather forecast model. In the model, we analyzed some events which had heavy rainfall more than 5mm/10min in the urban area. We narrowed the calculation domain to 1 km and 200 m. Using initial data are that terrain data is 10-m grid DSM (Digital Surface Model) of the geospatial information authority of Japan, the ground surface data is 100 m of ministry of the environment and sea surface temperature of Tokyo bay is 1 km of NASA. We improved the results by using 3DVAR (Three-Dimensional Variational) data assimilation (Fig. 1(b)).

Future work, we will be able to observe more accurate data by setting some CDL at urban area and expect to improve weather forecasting.

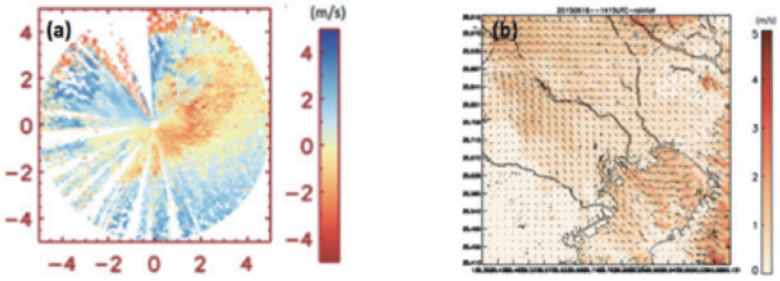

Fig .1 (a) Doppler lidar observation in Tokyo metropolitan area.
(b) Map of precipitation and wind distribution for numerical simulation.

References

[1] Seko, H., Miyoshi, T., Shoji, Y. and Saito, K.: Data assimilation experiments of precipitable water vapour using the LETKF system: intense rainfall event over Japan 28 July 2008, Tellus, Vol.63A, pp.402-414 (2011).
[2] Seko, H., Hayashi, S. and Saito, K.: Processes Generating Convection Cells near Sumatra Island in the Monsoon Season, Papers in Meteorology and Geophysics, Vol.63, pp.57-67 (2012).
[3] Skamarock, W. C., Klemp, J. B., Dudhia, J., Gill, D. O., Barker, D. M., Wang, W. and Powers, J. G.: A Description of the Advanced Research WRF Version3, NCAR TECHNICAL NOTE, p125 (2008).
[4] Wang, X., Barker, D. M., Snyder, C. and Hamill, T. M.: A Hybrid ETKF-3DVAR Data Assimilation Scheme for the WRF Model. Part Ⅰ: Observing System Simulation Experiment, Mon. Wea. Rev., Vol.136, pp.5116-5131 (2008a).
[5] Wang, X., Barker, D. M., Snyder, C. and Hamill, T. M.: A Hybrid ETKF-3DVAR Data Assimilation Scheme for the WRF Model. Part Ⅱ: Observing System Simulation Experiment, Mon. Wea. Rev., Vol.136, pp.5132-5147 (2008b).

ABSTRACTS (MASTER THESIS)

Optically transparent cotton composite and optical properties

**（Graduate School of Forest and Biomaterials science,
Laboratory of Active Bio-based Matesials, RISH, Kyoto University）**

Masahiro Morita

Introduction

In our previous studies, we investigated the preparation of optically transparent composites because CNFs don't cause light scattering in resin. It was found that a conventional purified pulp without aggregation of the cellulose microfibrils also become transparent by resin impregnation because cell walls of a plant primarily is composed with cellulose microfibrils[1)]. In this work, we focused on high cellulose content, crystallinity of the cotton fiber and its three-dimensional processability. The cotton fiber is also expected to become transparent but the cellulose microfibrils in the cotton fiber already aggregated. We tried to make the optically transparent cotton fiber composite with swelling between the cellulose microfibrils by tempo-oxidation treatment[2)] and surface acetylation of the cellulose microfibrils. Furthermore, we investigated that the acetylated cotton in toluene exhibited blue.

Experimental

Cotton powder was stirred in 16% NaOH for 24h(Mercerization). The mercerized cotton was tempo-oxidized at pH10 and then acetylated with acetic anhydride, perchloric acid, acetic and toluene after solvent exchange to acetic acid. Degree of substitution of the mercerized tempo-oxidized acetylated cotton(MTAC) was determined by titration. DS of carboxyl group and acetyl group were respectively adjusted to 0.55, 1.02. MTAC sample was dispersed in water and filtered by mesh. The mats of MTAC was hot-pressed at 105℃ and 0.17MPa. The dried sheet was impregnated with acrylic monomer in vacuum oven. The resin impregnated sheets were cured by UV. The MTAC composite sheets thus obtained were 119 μm thick, and its fiber content was about 40%.

Results and discussion

Compared with the untreated cotton, the mercerized tempo-oxidized cotton swelled in water and its slurry became transparent. It showed the swelling between cellulose microfibrils. The MTAC composite showed high transparency (Fig 1), because MTAC sheets was almost completely impregnated with acrylic resin. The MTAC reinforced composite showed low thermal expansion (Fig 2). In this case, the existence of cellulose crystals influenced the coefficient of thermal expansion. The cellulose crystals played an important role of reducing the thermal expansion of the acrylic resin. The acetylated cotton(DS:1.83) in toluene increased transparency and exhibited blue color. For the phenomenon, the regular light transmittance of the acetylated cotton toluene slurry decreased in the region of wavelength of blue color but it showed the constant light reflectance, regardless of the wavelength of the visible light. Therefore, the acetylated cotton in toluene selectively scattered the light of the wavelength of blue color. Moreover, the wavelength of the scattering light changed with depending on the refractive index of solvents. Consequently, the color of the acetylated cotton in the solvents changed. The acetylated cotton in the solvents behaved as the optical filters for the specific wavelength of the light.

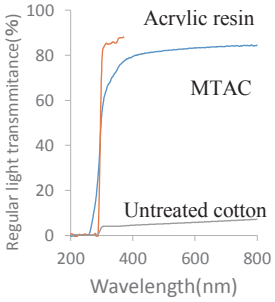

Figure 1. Transparency of composites

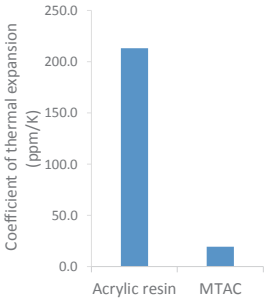

Figure 2. CTE of composite

References

1) H. Yano, et al., Adv. Optical Mater. **2**, 231-234, 2014.
2) M. Hirota, et al., Cellulose, **19**, 435-442, 2012.

ABSTRACTS (MASTER THESIS)

Investigation of new natural adhesives from sugars and phosphate compounds and applications to particleboard

**(Graduate School of Agriculture,
Laboratory of Sustainable Materials, RISH, Kyoto University)**

Shin Hayashi

Currently, wood-based materials were made by bonding between wood elements with synthesis resin adhesives. However, synthetic resin adhesives are mainly produced from fossil resources, and which lead to environmental load and depletion of fossil resources. Therefore, it is desirable to replace to natural-based adhesives based on non-fossil resources. Conventional natural adhesives have some issues such as complicated preparation, low water resistance. Recently it was found that mixed aqueous solution of sugar and phosphate compound had a potential to be used as an adhesive for wood.

In this study, mixtures using six types of sugars and four kinds of phosphate compounds were prepared, and the curing properties and bonding properties were clarified. The effects of type of sugars and phosphate compounds, mixture ratios and heating conditions on the curing properties were examined by thermal analyses, insoluble matter and FT-IR analysis. Furthermore, based on the results obtained, particleboards bonded with sugar and phosphate compound were prepared by changing the mixture ratio of the sugar and phosphate compound, hot press temperature and time and resin content. Some tests referring to JIS A 5908 were performed to evaluate physical properties and clarity preferable production conditions as well as the adhesive performance.

Preferable sugar and phosphate compound were sucrose and ammonium dihydrogen phosphate (ADP), respectively. The sufficient curing condition of the mixture of sucrose and ADP was temperature of 180℃ and time of 10 minute. The particleboard bonded with sucrose and ADP as an adhesive had excellent mechanical properties, water and decay resistances. The mechanical properties and water resistance of the boards satisfied with JIS standard and were comparable to those of the particleboards bonded with synthetic resin adhesives. Preferable production conditions were mixture ratio of sucrose and ADP of 85/15, press temperature of 200℃, press time of 10 minutes and resin content of 20 wt%. Consequently, it was clarified that the mixture of sucrose and ADP had good bonding properties and could be used as a natural adhesive.

ABSTRACTS (MASTER THESIS)

A study on destruction behavior of CLT wall with openings subjected in-plane shear force

**(Graduate School of Agriculture,
Laboratory of Structural Function, RISH, Kyoto University)**

Mami Wada

Cross Laminated Timber is a new structural panel element consist of several layers of structural lumber boards stacked crosswise (typically at 90 degrees) and glued together. In Japan, the CLT has attracted attention of architects recently due to its environment friendly characteristics and the expectation of .light weight and low cost construction style. Although material standard of CLT has been published, CLT structural design criteria for allowable stress design method is still under discussion. Currently two CLT construction methods has been proposed in Japan. One is the method using the big panels with the openings, and the other is the method using the small panels of about 1x3m in size connected together by the metal fasteners. This paper discuss about the former method. Although using the big panel with openings enables logical construction, there has been a difficulties in the estimation of stiffness and strength. Especially the behavior of the corner panel zone has not been clarified yet. Therefore in this study, the horizontal loading test was carried out to make clear the specific destruction behavior of the corner of big CLT panels, and to lead estimation formulas of stiffness and strength.

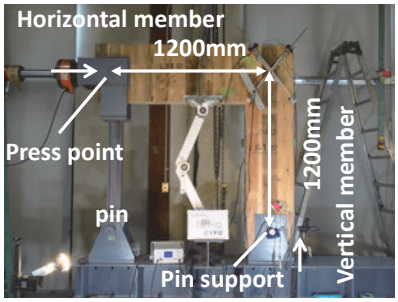

Figure 1. L-shaped CLT specimen

Experimental method and result

L and T-shaped specimens were cut out from large size CLT panels made of 5 layered Sugi laminae in Mx60B standard grade. While the specimens were fixed by the pin support, the horizontal load was applied and the relationship between moment and rotation angle at panel-zone was measured. Three kinds of loading schedules which were monotonic push over, monotonic pull over and cyclic loading were performed as parameter. In terms of L-shaped specimens, the most of pull specimens failed in bending at nearby the corner of panel zone and the most of cyclic specimens showed similar failure mode to pull specimens. As a result, the strength showed a big variation and its average value was different to the average of the bending test of straight CLT made of the same grade. From strain gauge measurement, followings were found. A non-side-bonding of lamina causes relative slip of laminas, and it was found that CLT plane section holding does not maintain. And the strain gages put near the inside-corner showed sever stress concentration. Those caused the low strength of pull specimens. As the specific failure mode, rolling-shear failure was observed in most of push specimens. It was thought caused by 3-dimentional stress transition via bonding surface of layers.

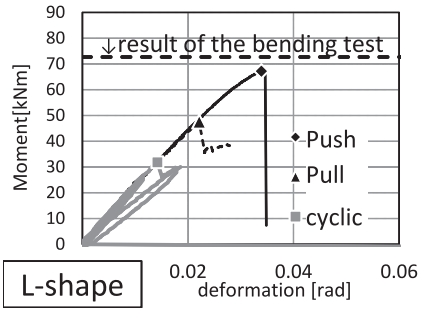

Figure 2. M-θ relationship (L-shaped CLT)

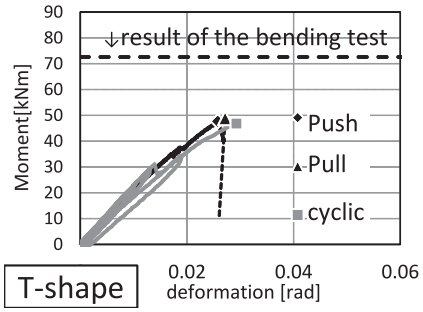

Figure 3. M-θ relationship (T-shaped CLT)

Conclusion

CLT L and T-shaped specimen tests revealed the specific behavior. The reason was partly clarified by the stress analysis and strain measurements. It is concluded the precise estimation of bending failure is important to design CLT building in the safer side.

ABSTRACTS (MASTER THESIS)

Study on Microwave Propagation for Wireless Sensor System in Car Engine Compartment

(Graduate School of Engineering, Laboratory of Applied Radio Engineering for Humanosphere, RISH, Kyoto University)

Hiroki Goto

Recently, a large number of sensors are installed in vehicles to monitor their conditions. However, the power wires for these sensors increase the vehicle's weight. To solve the weight increase problem, a microwave power transfer system is proposed as one of the management systems, which can provide electric power with sensors without the wires. In this paper, we investigated microwave propagation for wireless sensor system in car engine compartment. The maximum consumption power of the sensor is 100mW and the power of the Tx antenna is 500 mW from the limit of usable power in the engine control unit. We assumed the rf-dc conversion efficiency as 70%. Therefore, 140mW is necessary for the rectenna input. Then our target of the transmission efficiency is set to 28%.

First, we designed 2.45 GHz and 900 MHz antennas as Tx and Rx antennas. Then, we simulated and measured the antenna characteristics. Second, we simulated and measured the transmission efficiency in a simple engine compartment model. When Tx antenna faced Rx antenna, we confirmed the transmission efficiency in the simple engine compartment became larger than that in free space. The transmission efficiency at 900 MHz became larger than that at 2.45 GHz. In addition, we examined the transmission to the plural points or the over-the-horizon condition in the simple engine compartment model. Finally, we simulated and measured the transmission efficiency in a real engine compartment model. We changed the direction of the Tx and Rx antennas in the over-the-horizon condition, and obtained the simulation result of 2.8% and the measurement result of 1.2%. To improve the transmission efficiency, we simulated the transmission efficiency when Tx antenna faced Rx antenna. As a result, we obtained more than 28% of the transmission efficiency at 900 MHz when we used a dipole antenna with a reflector for Tx and Rx with a distance of 18 cm.

Acknowledgements

Part of this research was carried out by use of Microwave Energy Transmission Laboratory (METLAB) as collaborative inter-university research facility. Part of this research was supported by Denso corporation

ABSTRACTS (MASTER THESIS)

Study on High Power Rectifier with GaN Schottky Barrier Diode

**(Graduate School of Engineering,
Laboratory of Applied Radio Engineering for Humanosphere, RISH, Kyoto University)**

Takaki Nishimura

In these days, the demand on a microwave high power transfer system is increasing. In order to realize a high power transfer system via microwave, a diode used for a rectifier of the receiving device is necessary to have a high breakdown voltage and be operated at a high frequency of GHz class. The purpose of this study is to develop a high power rectifier that has 70% of the RF-DC conversion efficiency (η) at several ten watts of the input power (Pin), with a GaN schottky barrier diode that has about 100 V of the breakdown voltage. The frequency of the microwave is 2.45 GHz.

First, rectifiers with packaged diodes were simulated. In the simulation results, 76% of η was obtained at 27 W of Pin. Then, the rectifiers were fabricated and experimented. As a result, 43% of η was achieved at 7 W of Pin. At more than 7 W of Pin, the diode was broken by overheat.

Next, diodes with AlN submounts were used in order to improve the heat radiation characteristics. In the simulation, 71% of η was gained at 20 W of Pin. In the experiment, 40% of η was achieved at 20 W of Pin. When Pin was larger than 20 W, a wire between the circuit and the diode was broken by a large current. With the submount diodes, the maximum Pin of the rectifier could be successfully 13 W larger than that with the packed diodes. However, there remained 31% efficiency difference between simulations and experiments.

Finally, in order to improve η in the experiments, a line length that was series to the diode (x) was investigated because x was adjusted in the previous experiments. Rectifiers with the submount diodes were simulated with changing x from 0 mm to 42.2 mm. 42.2 mm was the half wave length. As a result, η changed with a cycle of λg/4. Then, rectifiers were experimented with changing x. As a result, 45% of η was achieved at 20 W of Pin. It was succeeded to improve 5% of η in the experiments.

Acknowledgements

Part of this research was carried out by use of Microwave Energy Transmission Laboratory (METLAB) as collaborative inter-university research facility. Part of this research was supported by Sumitomo Electric Industries, Ltd.

ABSTRACTS (MASTER THESIS)

Study on Receiving Antennas and Safety in Microwave Power Supply System to Vehicle Roof

**(Graduate School of Engineering,
Laboratory of Applied Radio Engineering for Humanosphere, RISH, Kyoto University)**

Yu Tsukamoto

We propose a wireless power supply system to the roof of an electric vehicle by using microwave power transfer. Since the system radiates high power microwaves, the unwanted microwave leakage outside of the system must be suppressed for human safety. The leakage is mainly caused by the microwave reflection on the receiving antennas. In this thesis, we analyze the receiving antennas to suppress the reflection.

In addition, it is also necessary to ensure the safety under unexpected situations. We discuss the safety of the system based on the detection devices against the situations. In order to evaluate the microwave reflection on the receiving antennas, the receiving efficiency of the system was investigated. First, the operation of dipole array antennas with reflector for plane wave incidence was analyzed by using FDTD method. The results clarified the effects of mutual coupling on the receiving efficiency, and the receiving efficiency of infinite array antenna reached 99.9% under the matching condition including the effects of mutual coupling. In order to simulate a practical case, we analyzed 12x12 array antenna performances under Gaussian-type microwave incidence. As a result, the receiving efficiency reached 99.9%, and the total microwave leakage outside of the system was reduced to 0.673%. Next, the receiving efficiency was experimentally evaluated. A plane wave was transmitted to 3 x 3 microstrip array antennas to measure the receiving efficiency. The results showed that the receiving efficiency was 77.8% with the element intervals of 0:4λ, and that of 0:5λ was 85.1%. For human safety, the power transmission must be stopped immediately by the detection devices under the unexpected situations. The response speed of the detection devices was measured for the situations of 1) inclined transmitting antennas, 2) object incursion into the transmitted beam. The experimental results clarified the conditions to ensure the safety for the situations.

Acknowledgements

Part of this research was carried out by use of Microwave Energy Transmission Laboratory (METLAB) as collaborative inter-university research facility. Part of this research was supported by Volvo corporation.

ABSTRACTS (MASTER THESIS)

An Investigation of Space-Based Space Debris Observation System

(Graduate School of Engineering, Laboratory of Space Systems and Astronautics, RISH, Kyoto University)

Naoya Iwanaga

Recently, the human activity in space is exposed to the menace of the dramatic increase of space debris. We know the position and the velocity of the debris over10cm, however we don't know the shape of them in detail. There are some assumption that many small debris under 10cm exist at an altitude of 800km -850 km, however there are no effective ways to detect them because of the resolution of the radar on the ground and the weather. Our purpose is to develop the system of debris observation satellite in order to estimate the shape and the orbit of known debris and unknown debris under 10cm around the Earth by observing in space.

In this paper, we focus on the three different factors of the debris observation satellite. The first one is the orbit. I choose the orbit of the debris observation satellite as Sun-synchronous orbit. The satellite is not influenced by the heat of sunlight in Sun-synchronous orbit. Moreover, if the direction of the sensor is held toward the opposite of the Earth, I can reduce the heat of sunlight and the Earth. The second one is the altitude. I consider the altitude of the debris observation satellite where I can find more space debris. If I choose the altitude of the satellite to be under that of 800km -850 km, I can reduce the possibility of a collision with space debris. On the other hand, the satellite cannot find space debris clearly because it is far from space debris. The third one is the equipment. I consider two kinds of the sensor for the debris observation satellite, an optical sensor and a laser radar sensor. An optical sensor observes space debris by perceiving visible rays or near infrared ray. A laser radar sensor uses a laser beam in order to investigate space debris. This detects the space debris by receiving the scattered light of space debris. Moreover, a laser radar sensor can get the velocity of space debris by the Doppler beat. If I assume the parameter of the debris and the capacity of the sensor, I can decide the distance between the satellite and the observable debris.

We will discuss the effective way of debris observation in detail and the possibility of space debris observation via satellites.

ABSTRACTS (MASTER THESIS)

Study on Observation Plan for Space Debris Using the MU Radar

(Graduate School of Engineering, Laboratory of Space Systems and Astronautics, RISH, Kyoto University)

Kazuki Masunari

The purpose of this study is to develop appropriate observation plans for the effective observation of identified and unidentified space debris. We used the MU radar as an observatory of the debris.

As to the identified debris, we can get information about their orbital elements as two-line elements (TLE). We made an observation plan by calculating debris' orbits from TLE and relative positions to the MU radar. Based on the organized plan, we observed debris with the MU radar. According to the plan, six debris can be observed with the MU radar, and as a result of the observation, we identified signals of debris from all observed data. The time errors between the estimated time of the organized plan and measured one were within 10 seconds. Furthermore, concerning range, the organized plan was accurate. Thus, the method of planning we used in observing the debris was verified as reliable for the debris observation.

As to the unidentified debris, which will be generated from explosions and collisions of space satellites in the future, we proposed an observation plan by estimating debris' orbit for 72 hours from the generation and the direction in which more debris pass. To assume more realistic conditions, we reproduced past two accidents of satellites which generate debris in this study. As a result of calculation, we found the deviation of the debris to particular directions.

In the present study, as to the identified debris, we proved the reliability of our observation plan by the observations with the MU radar. As to the unidentified debris, we proposed a method of planning by simulating the real fragmentation accidents. Evaluating the validity of the method we proposed for the unidentified debris is our future work.

ABSTRACTS (MASTER THESIS)

Study on Miniaturization of Particle Detection Circuits Composing the Direct Observation System for Wave-Particle Interactions

(Graduate School of Engineering, Laboratory of Space Systems and Astronautics, RISH, Kyoto University)

Keisuke Onishi

"Wave-Particle Interaction Analyzer (WPIA)" is proposed for a direct and quantitative analysis of wave-particle interactions. We aim to integrate the WPIA on one-chip by using the ASIC (Application Specific Integrated Circuits). In order to realize the one-chip WPIA, small-size particle detection circuits are required which continuously output a detection signal derived from each plasma particle. This thesis describes the design and evaluation of the small particle detection circuit on a chip.

The operation of the particle detection circuit consists of two stages. Since the plasma particle cannot be detected directly, the pre-stage converts and amplifies electric charge detected by a sensor to voltage first, enabling the post-stage to detect the voltage signal. The input waveform to the pre-stage circuit appears as a current pulse with its pulse width of a few tens of nano-seconds. In order to keep an enough response to the short time pulse in converting the electric charge to the voltage, we chose a current conveyor and a latch comparator for the pre-stage and post-stage circuits, respectively. First, we designed a current conveyor. The response of the current conveyor depends on mutual conductance (g_m) of MOSFETs and the output impedance (Z_{out}). With a large value of g_m and Z_{out}, we designed a high response current conveyor circuit. Simulation results show that when the amplitude of the input current pulse was 103 μA, the output was raised from -12.7 mV to 316 mV at about 1.8 ns and converged at about 16.2 ns. The operational performance of the current conveyor circuit was also verified by the measurement and simulation results. Next, we designed a latch comparator. Adjusting the current and the aspect ratio of MOSFETs on the latch circuit, we designed a high response latch comparator with the delay time of less than 2 ns. The measurement results, however, showed the delay time of about 200 ns, due to the time constant increased by parasitic capacitance at the output port, which was improved by decreasing Z_{out} in simulation. Finally, we proposed a direct observation system for wave-particle interactions including the designed particle detection circuits.